WNT Signaling Perturbations Underlie the Genetic Heterogeneity of Robinow Syndrome

Janson J. White,[1] Juliana F. Mazzeu,[2,3] Zeynep Coban-Akdemir,[1] Yavuz Bayram,[1] Vahid Bahrambeigi,[1,4] Alexander Hoischen,[5,6] Bregje W.M. van Bon,[5] Alper Gezdirici,[7] Elif Yilmaz Gulec,[7] Francis Ramond,[8] Renaud Touraine,[8] Julien Thevenon,[9,10,11] Marwan Shinawi,[12] Erin Beaver,[13] Jennifer Heeley,[13] Julie Hoover-Fong,[14] Ceren D. Durmaz,[15] Halil Gurhan Karabulut,[15] Ebru Marzioglu-Ozdemir,[16] Atilla Cayir,[17] Mehmet B. Duz,[18] Mehmet Seven,[18] Susan Price,[19] Barbara Merfort Ferreira,[2] Angela M. Vianna-Morgante,[20] Sian Ellard,[21,22] Andrew Parrish,[21] Karen Stals,[21] Josue Flores-Daboub,[23] Shalini N. Jhangiani,[24] Richard A. Gibbs,[1,24] Baylor-Hopkins Center for Mendelian Genomics, Han G. Brunner,[25,26] V. Reid Sutton,[1,27] James R. Lupski,[1,24,27] and Claudia M.B. Carvalho[1,*]

Locus heterogeneity characterizes a variety of skeletal dysplasias often due to interacting or overlapping signaling pathways. Robinow syndrome is a skeletal disorder historically refractory to molecular diagnosis, potentially stemming from substantial genetic heterogeneity. All current known pathogenic variants reside in genes within the noncanonical Wnt signaling pathway including *ROR2*, *WNT5A*, and more recently, *DVL1* and *DVL3*. However, ~70% of autosomal-dominant Robinow syndrome cases remain molecularly unsolved. To investigate this missing heritability, we recruited 21 families with at least one family member clinically diagnosed with Robinow or Robinow-like phenotypes and performed genetic and genomic studies. In total, four families with variants in *FZD2* were identified as well as three individuals from two families with biallelic variants in *NXN* that co-segregate with the phenotype. Importantly, both *FZD2* and *NXN* are relevant protein partners in the WNT5A interactome, supporting their role in skeletal development. In addition to confirming that clustered –1 frameshifting variants in *DVL1* and *DVL3* are the main contributors to dominant Robinow syndrome, we also found likely pathogenic variants in candidate genes *GPC4* and *RAC3*, both linked to the Wnt signaling pathway. These data support an initial hypothesis that Robinow syndrome results from perturbation of the Wnt/PCP pathway, suggest specific relevant domains of the proteins involved, and reveal key contributors in this signaling cascade during human embryonic development. Contrary to the view that non-allelic genetic heterogeneity hampers gene discovery, this study demonstrates the utility of rare disease genomic studies to parse gene function in human developmental pathways.

Introduction

The study of rare disease informs human biology. Bridging the gap between disease and gene can often provide the initial insights into gene function and disease mechanism, drive experimental clinical or laboratory questions, and provide immediate practical application in clinical genomic dignostics.[1] Robinow syndrome (RS) is a congenital skeletal dysplasia, with autosomal-dominant (DRS) and -recessive (RRS) inheritance and evidence for genetic heterogeneity. Originally described by Meinhard Robinow in 1969, it is characterized by short stature, mesomelic limb shortening, broad thumbs and toes, genital hypoplasia, and distinctive and recognizable craniofacial features with frontal bossing, high, broad forehead, depressed nasal bridge, and prominent eyes; the tall forehead relative to the face leads to facial disproportion often termed the "fetal face."[2] The clinically more severe recessive Robinow syndrome (RRS [MIM: 268310]) has been associated with biallelic variants in the tyrosine kinase-like orphan receptor,

[1]Department of Molecular and Human Genetics, Baylor College of Medicine, Houston TX 77030, USA; [2]University of Brasilia, Brasilia 70910, Brazil; [3]Robinow Syndrome Foundation, Anoka, MN 55303, USA; [4]Graduate Program in Diagnostic Genetics, School of Health Professions, University of Texas MD Anderson Cancer Center, Houston, TX 77030, USA; [5]Department of Human Genetics, Radboud Institute of Molecular Life Sciences, Radboud University Medical Center, 6500 HB Nijmegen, the Netherlands; [6]Department of Internal Medicine and Radboud Center for Infectious Diseases (RCI), Radboud University Medical Center, 6500 HB Nijmegen, the Netherlands; [7]Department of Medical Genetics, Kanuni Sultan Suleyman Training and Research Hospital, Istanbul 34303, Turkey; [8]Service de Génétique, CHU-Hôpital Nord, 42000 Saint-Etienne, France; [9]Inserm UMR 1231 GAD team, Genetics of Developmental Anomalies, Université de Bourgogne-Franche Comté, 21000 Dijon, France; [10]FHU-TRANSLAD, Université de Bourgogne, 21000 CHU Dijon, France; [11]Centre de génétique, Hôpital Couple-Enfant, CHU de Grenoble-Alpes, 38700 La Tronche, France; [12]Division of Genetics and Genomic Medicine, Department of Pediatrics, Washington University School of Medicine, St. Louis, MO 63110, USA; [13]Mercy Clinic-Kids Genetics, Mercy Children's Hospital St. Louis, St. Louis, MO 63141, USA; [14]Greenberg Center for Skeletal Dysplasias, McKusick-Nathans Institute for Genetic Medicine, Johns Hopkins University, Baltimore, MD 21287, USA; [15]Department of Medical Genetics, Ankara University School of Medicine, 06100 Ankara, Turkey; [16]Department of Medical Genetics, Erzurum Regional and Training Hospital, 25070 Erzurum, Turkey; [17]Erzurum Training and Research Hospital, Department of Pediatric Endocrinology, 25070 Erzurum, Turkey; [18]Department of Medical Genetics, Cerrahpasa Medical School, Istanbul University, 34452 Istanbul, Turkey; [19]Oxford Centre for Genomic Medicine, Nuffield Orthopaedic Centre, Oxford OX3 7LD, UK; [20]Department of Genetics and Evolutionary Biology, Institute of Biosciences, Sao Paulo - SP 05508-090, Brazil; [21]Department of Molecular Genetics, Royal Devon and Exeter NHS Foundation Trust, Exeter EX2 5DW, UK; [22]Institute of Biomedical and Clinical Science, University of Exeter Medical School, Exeter EX1 2LU, UK; [23]Department of Pediatric Genetics, University of Utah School of Medicine, Salt Lake City, UT 84108, USA; [24]Human Genome Sequencing Center, Baylor College of Medicine, Houston, TX 77030, USA; [25]Department of Human Genetics, Donders Institute for Brain, Cognition and Behaviour, Radboud University Medical Center, 6500 HB Nijmegen, the Netherlands; [26]Department of Clinical Genetics, GROW School for Oncology and Developmental Biology, Maastricht University Medical Center, 6202 AZ Maastricht, the Netherlands; [27]Texas Children's Hospital, Houston, TX 77030, USA
*Correspondence: cfonseca@bcm.edu
https://doi.org/10.1016/j.ajhg.2017.10.002.

ROR2 (MIM: 602337), in an estimated 80% of the case subjects described.[3,4] *ROR2* is essential for noncanonical Wnt (β-catenin-independent) signaling that establishes cellular orientation via the Wnt/planar cell polarity pathway (PCP).[5] Ensuing discovery of heterozygous hypomorphic missense alleles in *WNT5A* (MIM: 164975), the gene that encodes the signal transducer and the putative ligand for ROR2, resulting in dominant Robinow syndrome (DRS1 [MIM: 180700]),[6] supports the hypothesis that a specific pathway could be involved in the disease etiology. More recently, *de novo* indels resulting in clustered protein-truncating variants affecting two out of the three human orthologs of the *Drosophila dishevelled* (*dsh*) gene, *DVL1* and *DVL3* (MIM: 601365, 601368), were shown to be another cause of dominant Robinow syndrome (DRS2 [MIM: 616331], DRS3 [MIM: 616894]).[7–9] This finding is consistent with the observation that human genes with two or more paralogs for the *Drosophila* ortholog are eight times more likely to be disease relevant.[10] DVL is a key downstream mediator of the Wnt pathway, including the Wnt/noncanonical PCP pathway via interaction with ROR2,[11,12] which further strengthens the link of the disease with a perturbed PCP signaling cascade during human development.

The mutational mechanism observed in *DVL1*- and *DVL3*-associated RS is exclusively clustered mutations in the penultimate or last exon resulting in −1 frameshifting variants that result in a premature stop codon within the last exon. Those variants generate a stable mRNA that is predicted to translate into a mutant protein with a similarly truncated C terminus. This is remarkably specific and recurs independently in DRS-affected families.[7–9] Whether the pathogenicity of these truncated proteins results from a gain-of-function or dominant-negative effect is actively being investigated, but preliminary experimental data suggest that it is not driven by the loss of the C terminus alone.[8] Collectively, the pathogenesis of RS appears to be a result of perturbation of the WNT5A/ROR2 signaling cascade required for efficient PCP.

The Wnt signaling pathways control many critical early developmental and post-natal physiological processes. One fundamentally important function of noncanonical Wnt signaling is to provide directional information by regulating the evolutionarily conserved PCP pathway. The PCP pathway is essential for vertebrate embryogenesis, including convergent-extension movements and limb bud outgrowth and patterning.[13] The core system of Wnt/PCP signaling is composed of a set of highly conserved proteins that interact with each other to form opposing complexes at opposite sides of the cell, thus allowing cellular orientation.[14] Mutation in genes crucial for PCP have been linked to human diseases, including neural tube defects[15,16] and nearly identical mouse phenotypes,[17,18] most notably RS.[3,6,7,9] Moreover, despite discovery of some of the genes and variants underlying DRS, it is estimated that 70% to 80% of individuals with DRS have an unknown underlying molecular etiology.[7,9] Based on the fact that all the Robinow syndrome-associated proteins play a vital role in noncanonical Wnt/PCP signaling, we hypothesized that studying subjects with Robinow syndrome would reveal other causative variants within genes important to the establishment of PCP and human development.

Herein we report the analyses of a Robinow syndrome-affected cohort where we applied a combination of targeted Sanger and whole-exome sequencing (WES) studies to 21 unrelated families diagnosed clinically with RS, some of whom have more than one individual affected. This study revealed *de novo* and/or private variants affecting four genes for which translated proteins directly interact with DVL1 and DVL3 or have a role in the Wnt/PCP pathway: *FZD2* (MIM: 600667), *NXN* (MIM: 612895), *RAC3* (MIM: 602050), and *GPC4* (MIM: 300168). Importantly, mutations of the Frizzled receptor, FZD2, alone accounts for 3/21 (14%) of the clinically ascertained RS-affected case subjects, two of which are due to substitution of an identical amino acid that maps adjacent to the domain that directly interacts with DVL. In addition, we report that *NXN*, which encodes a regulator of the Wnt pathway, is also associated with RRS.[19,20] In total, *WNT5A*, *DVL1*, *DVL3*, and *FZD2* explain 12/21 (57%) of our DRS-affected case subjects. In summary, these data strongly support the notion that RS results from perturbation of the Wnt/PCP pathway during human development and reveals specific gene paralogs, key proteins, and potential domains involved in human limb and craniofacial formation.

Subjects and Methods

Study Participants

We recruited 21 unrelated individuals with a clinical diagnosis of RS or presenting clinical features consistent with a Robinow-like syndrome. Of the 21 probands, 10 were ascertained during the 13th Biennial Robinow Syndrome Conference in Minneapolis, MN. All individuals were screened for pathogenic variants in *ROR2* before inclusion into this study, and therefore the cohort was biased toward individuals with the dominant form of RS. Inclusion was based on core clinical phenotypes including characteristic facial features, short stature, and limb abnormalities but not altogether meeting a strict criterion for DRS clinical diagnosis (see Supplemental Note for detailed clinical synopsis). RS was of sporadic occurrence, except for two families with an affected mother and child. DNA was obtained after all relevant family members provided written informed consent. Two additional families, which were not included in the original cohort, were subsequently ascertained via GeneMatcher. This study was approved by the institutional review board at Baylor College of Medicine (protocol no. H-29697).

Sanger Sequencing

From our previous studies, we estimate that nearly 20% of DRS results from truncating alleles in either *DVL1* or *DVL3*.[7,9] Therefore, before performing WES, we first Sanger sequenced the penultimate and final exons of *DVL1* and *DVL3* from the 21 probands, since DVL-mediated RS is the unique result of clustered −1 frameshifting indels in either *DVL1* or *DVL3*, the mRNAs being predicted to escape nonsense-mediated decay.[7,9] All PCR products containing candidate frameshift alleles detected by Sanger

sequencing were further confirmed using allele-specific sequencing via manually cloning both alleles into a standard TOPO TA cloning vector (Life Technologies) and then transforming the recombinant clones into chemically competent *Escherichia coli* to be grown overnight. Individual clonal colonies were then sequenced by a standard Sanger dideoxy capillary sequencing.

Exome Sequencing

The DNA samples from "unsolved" individuals lacking pathogenic variants in either *DVL1* or *DVL3* were subjected to WES, through the Baylor-Hopkins Center for Mendelian Genomics initiative.[21] WES was performed at the Baylor College of Medicine-Human Genome Sequencing Center (BCM-HGSC), and pre-captured libraries were pooled and then hybridized in solution using the BCM-HGSC in-house VCRome 2.1 design[22] according to the manufacturer's protocol *NimbleGen SeqCap EZ Exome Library SR User's Guide* with minor revisions. All samples achieved 96% of the targeted exome bases covered to a depth of 20× or greater with an average depth of coverage of 95× . The choice of variant annotation software can influence the filtering and parsing of rare variants, thus affecting one's ability to identify potential disease-relevant variants. Differing annotation software tools often provide distinct interpretations and varying levels of false-positive and false-negative findings; this appears particularly true for indels.[23] To maximize our variant discovery from the Illumina sequencing data, we used two variant discovery methods in parallel starting with the BCM-HGSC Mercury analysis pipeline,[24] which moves data from the initial sequence generation on the instrument to annotated variant call files (VCF) via various analysis tools. In addition, we used the Genome Analysis Toolkit (GATK) HaplotypeCaller to produce joint called files with indel realignment and base recalibration in all families that underwent WES. We identified *de novo* mutations *in silico* by using read-depth information extracted from the BAM files of either parent and proband using the in-house developed software DNM-Finder.[25] Candidate variants were filtered against exome data in publicly available databases, including the 1000 Genomes Project, the NHLBI Exome Sequencing Project (ESP) Exome Variant Server, the Atherosclerosis Risk in Communities Study (ARIC) database, and our internal Baylor-Hopkins Centers for Mendelian Genomics variant analyzer database of approximately 6,400 exomes. In addition, all affected individuals were screened for copy-number variants (CNV) with exome data, utilizing XHMM[26] and our in-house developed algorithm for detecting homozygous exonic deletions, HMZDelFinder.[27] We also used WES data to calculate a B-allele frequency and delineate genomic intervals for absence of heterozygosity consistent with identity by descent.[27] We verified and evaluated potential disease-associated variants identified via WES for co-segregation with the phenotype by using standard PCR amplification. PCR products were purified with ExoSAP-IT (Affymetrix) and sequenced with dideoxy nucleotide Sanger sequencing at the DNA Sequencing and Gene Vector Core at Baylor College of Medicine.

Results

Contribution of Genes Associated with Robinow Syndrome

We initially set out to confirm and assess the contribution of *DVL1* and *DVL3* to DRS by targeted Sanger sequencing of the penultimate and final exons in *DVL1* and *DVL3* from our in-house database of clinically diagnosed RS-affected subjects (n = 21). Seven individuals (33%) presenting with DRS harbored likely pathogenic variants in either *DVL1* or *DVL3*, offering strong support to our assertion that at least 20% of DRS are caused by indels in *DVL1* or *DVL3*. The identified variants in *DVL1* and *DVL3* are shown in Figures 1A, 1B, S1, and Table S1. Five individuals had truncating alleles distributed within a highly GC-rich, 116-nucleotide stretch of the penultimate exon of *DVL1* according to RefSeq transcript GenBank: NM_004421.2. Two unrelated individuals contained an identical 4-base-pair duplication (c.1612_1616dup [p.Ser539Argfs*112]), another individual harbored a single base-pair deletion (c.1623del [p.Ser542Valfs*107]), and one individual had a 16-base-pair deletion (c.1608_1623del [p.Ser537Valfs*107]). Lastly, two unrelated individuals contained distinct 13-base-pair deletions (c.1496_1508del [p.Pro499Argfs*146], c.1505_1517del [p.His502Profs*143]) located in a region where half (9/17) of all reported variants in *DVL1* are tightly clustered, likely the result of sequence complexity of this region. The repeated sequence "GCTGCCC" is potentially mediating the recurrently observed 13-bp deletion variants via secondary structure mutagenesis.[28] In total, the four newly identified pathogenic variants in *DVL1* are consistent with previous reports wherein variants are tightly clustered in the penultimate exon and result in a −1 frameshift.

In addition to the six subjects with variants in *DVL1*, one individual had a likely pathogenic variant in *DVL3*. According to the *DVL3* Refseq transcript GenBank: NM_004423.3, this variant is located in the penultimate exon (c.1617del [p.Gln539Hisfs*129]). Collectively, and in agreement with previous reports, the variants in *DVL1* and *DVL3* indicate that DVL-mediated RS is the unique result of clustered −1 frameshifting indels supporting the hypothesis that translation from this mutant reading frame is necessary for the pathogenic effect, due to either a gain-of-function or dominant-negative effect.[7–9]

The first gene to be associated with DRS was *WNT5A*, but hypomorphic missense alleles of *WNT5A* in DRS-affected individuals has only been reported in a small number of subjects with DRS (<10 individuals). All individuals without pathogenic variants in *DVL1* or *DVL3* were studied by WES and two likely pathogenic variants in *WNT5A* were found in two unrelated probands (Figure 1C). In addition to the annotated WES results, to ensure complete sequence read coverage, we manually visualized the coding regions of *WNT5A* in the Integrative Genomic Viewer (IGV) for all affected individuals studied. One individual, BAB9138, contained a private missense in *WNT5A* (GenBank: NM_003392.4; c.479C>G [p.Ser160Cys]), but this individual was adopted and parental studies to segregate this allele are unavailable. Another individual, BAB9131, was found to carry a *de novo* non-frameshift 6-base-pair insertion affecting *WNT5A* (GenBank: NM_003392.4; c.487_492dup [p.Gly163_Cys164dup]). The variant was

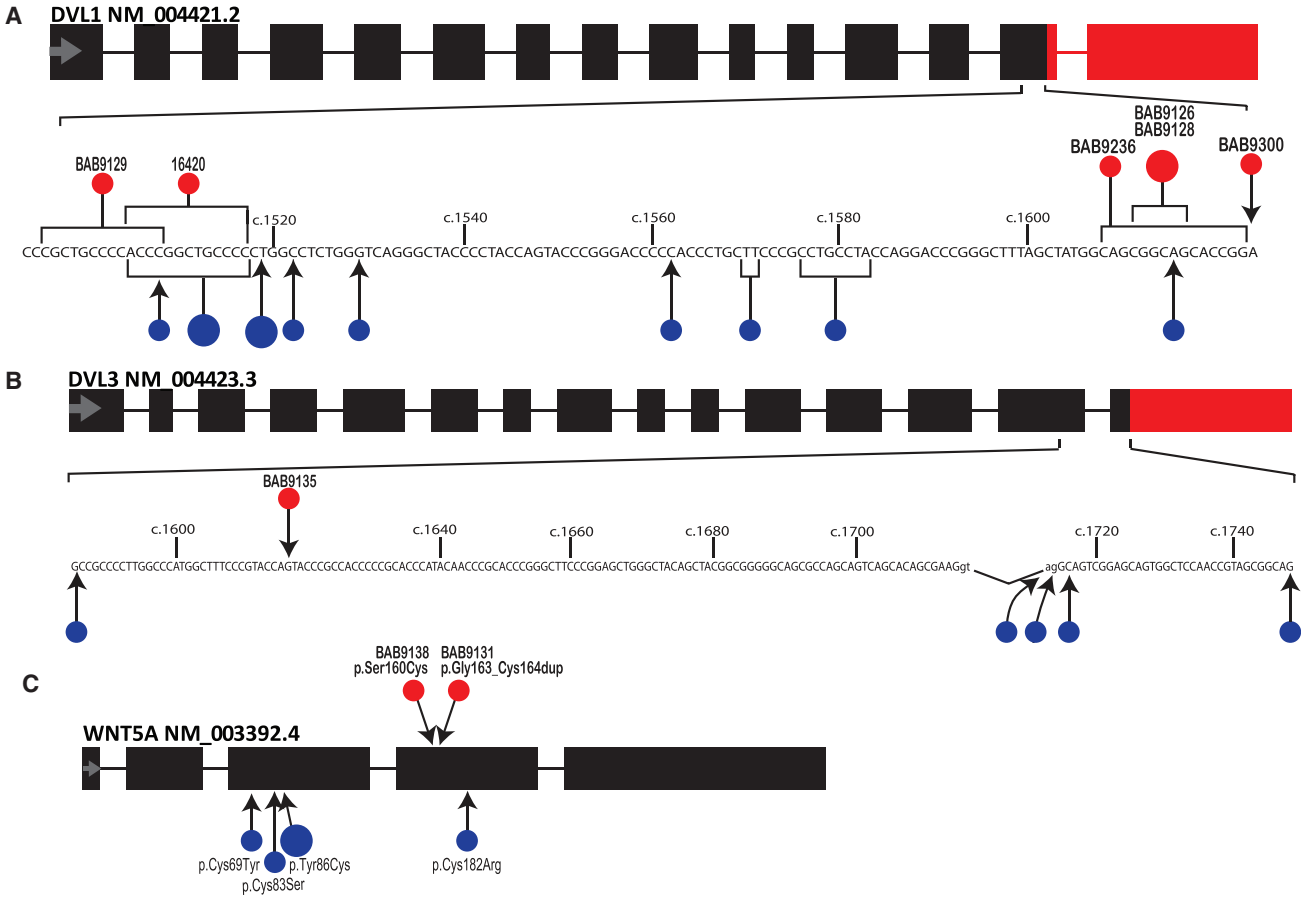

Figure 1. Location of Identified Variants in *DVL1*, *DVL3*, and *WNT5A* Resulting in Dominant Robinow Syndrome
The variants in *DVL1* and *DVL3* are mostly small insertions or deletions, except for two splicing variants in *DVL3*; all of them are predicted to lead to −1 frameshifting. Black rectangles represent transcript segments identical to the reference *DVL1* (A), *DVL3* (B), or *WNT5A* (C) mRNAs. Red rectangles indicate the shared transcript regions affected by the −1 frameshift in the predicted protein structure in all subjects. Part of exon 14 (*DVL1*) or exons 14 and 15 (*DVL3*) transcript sequence is shown in detail. Previously described variants are displayed by blue circles, whereas variants identified in this study are displayed by red circles. Larger circles represent identical variants in unrelated individuals. For complete description of all variants, see Tables S1 and S2.

observed in 16/70 (23%) mapped reads, which is consistent with a mosaic state of the mutant allele. The identification of only two individuals (~9.5%) in our cohort of 21 RS-affected probands indicates that *WNT5A* is an infrequent cause for this disorder. All publicly available pathogenic *WNT5A* variants are demonstrated in Figure 1C.[6,29]

The clinical phenotype of BAB9131 and BAB9138 were generally more severe than previous reports of individuals with WNT5A-mediated RS as both individuals presented with hemivertebrae and significant mesomelic limb shortening indicating that these variants, including one that appears to be mosaic in blood DNA, may result in a more severe RS phenotype (see Supplemental Note for the detailed clinical findings).

Differential Diagnosis of Robinow Syndrome

Approximately 57% of our cohort (12 out of 21) did not yield a pathogenic variant in *DVL1*, *DVL3*, or *WNT5A*. The remaining "unsolved" individuals were then studied by WES, thus allowing for gene discovery and a comprehensive and agnostic screening of all the genes within the broader differential diagnosis of clinical observations consistent with RS.

Clinical findings in subjects diagnosed with RS can elicit a range of potential differential diagnoses, including other skeletal disorders, most notably Aarskog-Scott syndrome (MIM: 305400), Opitz G/BBB syndrome (MIM: 145410), and omodysplasia type 2 (MIM: 164745). In our cohort, four individuals were found to carry likely pathogenic single-nucleotide variants (SNVs) in genes associated with diseases considered within the context of the differential clinical diagnoses of DRS. In addition, one individual, BAB8836, has two large copy-number variants that were revealed by XHMM and/or HMZDelFinder and further confirmed by aCGH (Figure S2). The CNVs are constituted by an ~8.3 Mb deletion of the short arm of chromosome X and a ~13 Mb duplication spanning the long arm of chromosome 6. Array analysis in parental samples indicates a *de novo* event but chromosome analysis did not reveal any visible cytogenetic abnormalities in the proband, which supports the hypothesis that BAB8836

carries an unbalanced chromosomal translocation; karyotype 46,XY,der(X)t(X;6)(p22.31;q25.3).arr[GRCh37] 6q25.3q27(157,870,814_170,881,475)x3, Xp22.33p22.31 (409,876_8,199,541)x0. Parental samples were not available for further testing so we could not rule out the possibility that BAB8836 has inherited an unbalanced chromosome translocation that resulted from the transmission of a derivative chromosome involved in a balanced event in the mother. The Xpter deletion encompasses the pseudoautosomal gene *SHOX* (MIM: 312865), deletion of which causes Leri-Weill dyschondrosteosis (MIM: 127300). The partial duplication of the long arm of chromosome 6 and the hemizygous deletion of Xpter also encompasses several known contiguous gene deletion syndromes including chondrodysplasia punctata (MIM: 302950) and ichthyosis (MIM: 308100). Collectively, the clinical phenotype of BAB8836 includes short stature, developmental delay, distal phalangeal hypoplasia, dryness of the skin, scoliosis, hemivertebrae, and an increase of sclerosis in bones, representing a unique amalgamation resulting from these large copy-number variants (see Supplemental Note).

Two male subjects, BAB8747 and BAB8751, were found to have hemizygous frameshift mutations in *FGD1* (GenBank: NM_004463.2; c.892dup [p.Cys298Leufs*5] and c.527dup [Leu177Thrfs*40]) (Table S1). Truncating alleles in *FGD1* (MIM: 300546) are an established cause of Aarskog-Scott syndrome, which has a wide phenotypic variability that largely overlaps with DRS. One individual, BAB8743, was found to have a previously reported pathogenic variant in *PTPN11* (MIM: 176876; GenBank: NM_002834.4; c.836A>G [p.Tyr279Cys]).[30] The resulting disorder, Noonan syndrome (MIM: 163950), often includes facial features similar to those of DRS.

Lastly, in BAB8759, who was the offspring of consanguineous parents, homozygous pathogenic variants were identified in two genes mapping to distinct segments of absence of heterozygosity (AOH) on heterologous chromosomes. A homozygous frameshift deletion was detected in *SH3PXD2B* (MIM: 613293; GenBank: NM_001017995.2; c.969del [p.Arg324Glyfs*19]). Recessive loss-of-function mutations in *SH3PXD2B* cause Frank-Ter Haar syndrome (MIM: 249420)[31] and multiple skeletal anomalies and heart defects which likely explain these clinical observations in subject BAB8759. Additionally, the homozygous missense variant in *INPPL1* (MIM: 600829; GenBank: NM_001567.3; c.1636G>A [p.Val546Ile]) likely contributes to the additional clinical features present in BAB8759, including nuchal edema and recurrent respiratory infections, which are observed in opsismodysplasia (MIM: 258480).[32] Therefore, the resulting clinical features of BAB8759 are likely a blended phenotype[33] resulting from a dual molecular diagnoses in which homozygous single gene defects in both *INPPL1* and *SH3PXD2B* contributed. From our cohort of 21 families, identification of one individual with a likely dual molecular diagnosis (4.8%) is consistent with previous estimates of the rate of dual molecular diagnosis in clinical WES.[33–35] In total, five individuals from our cohort of 21 families who were ascertained due to a clinical impression of RS were found to contain likely pathogenic variants in other relevant genes that represent a broad range of overlapping features. This demonstrates the utility of exome sequencing and molecular diagnosis as an adjuvant approach to achieve characterization of affected individuals as well as detecting disease-gene associations in a complex clinical landscape.[35,36]

Recurrent Missense and Truncating Variants in *FZD2* Cause Robinow Syndrome Features

Similar to the "solve-rate" for RS, after analyzing our cohort for known genes with a disease association, seven individuals from our cohort (7/21) remained without a molecular diagnosis. We then performed a personal genome analysis to identify rare and potentially damaging variants that might represent additional genes underlying DRS. Most notably, five affected individuals from three distinct families with DRS or Robinow-like traits had variants affecting *FZD2* either *de novo* or co-segregating with the disease. We then performed a GeneMatcher[37] search which led to the identification of a fourth family with a single simplex case of Robinow-like features and a *de novo* variant in *FZD2*. The four families, identified *FZD2* variants, and selected subjects are shown as Figure 2 and described in Table S1.

Of note, the same amino acid residue, glycine 434, is altered in three out of four families. One family with an affected mother and child co-segregate a missense variant (GenBank: NM_001466.3; c.1301G>T [p.Gly434Val]) and one subject has a dinucleotide substitution (c.1301_1302delinsTT [p.Gly434Val]), but the same modification at the protein level (Figures 2A–2C). Lastly, in one affected individual, a *de novo* variant (c.1300G>A [p.Gly434Ser]), which also changes the same codon, altering residue Gly434 was observed. Residue Gly434 is conserved throughout all vertebrates and is located at the edge of a transmembrane domain; the adjacent intracellular loop is one of the three motifs that were shown to be required for binding and stabilizing the interaction with Dvl1.[38] Therefore, alterations in Gly434 potentially interfere or enhance the affinity or stability of the FZD2-DVL interaction, which has been shown to occur via the C terminus of DVL1 including the DEP domain.[39]

In contrast to the above individuals with *FZD2* variants, one subject (BAB8596) carries a nonsense truncating allele (c.1130G>A [p.Trp377*]) in addition to a variant of uncertain significance (VUS) (c.425C>T [p.Pro142Leu]) affecting *FZD2* in *trans* (Figure 2). The nonsense single-nucleotide variant is located upstream of the recurrent variant present in all other families and is predicted to result in truncation of nearly 200 aa at the C terminus. *FZD2* is a single-exon gene not subject to nonsense-mediated decay, thus indicating that this truncating allele may produce a stable mRNA product. BAB8596 inherited this allele from his

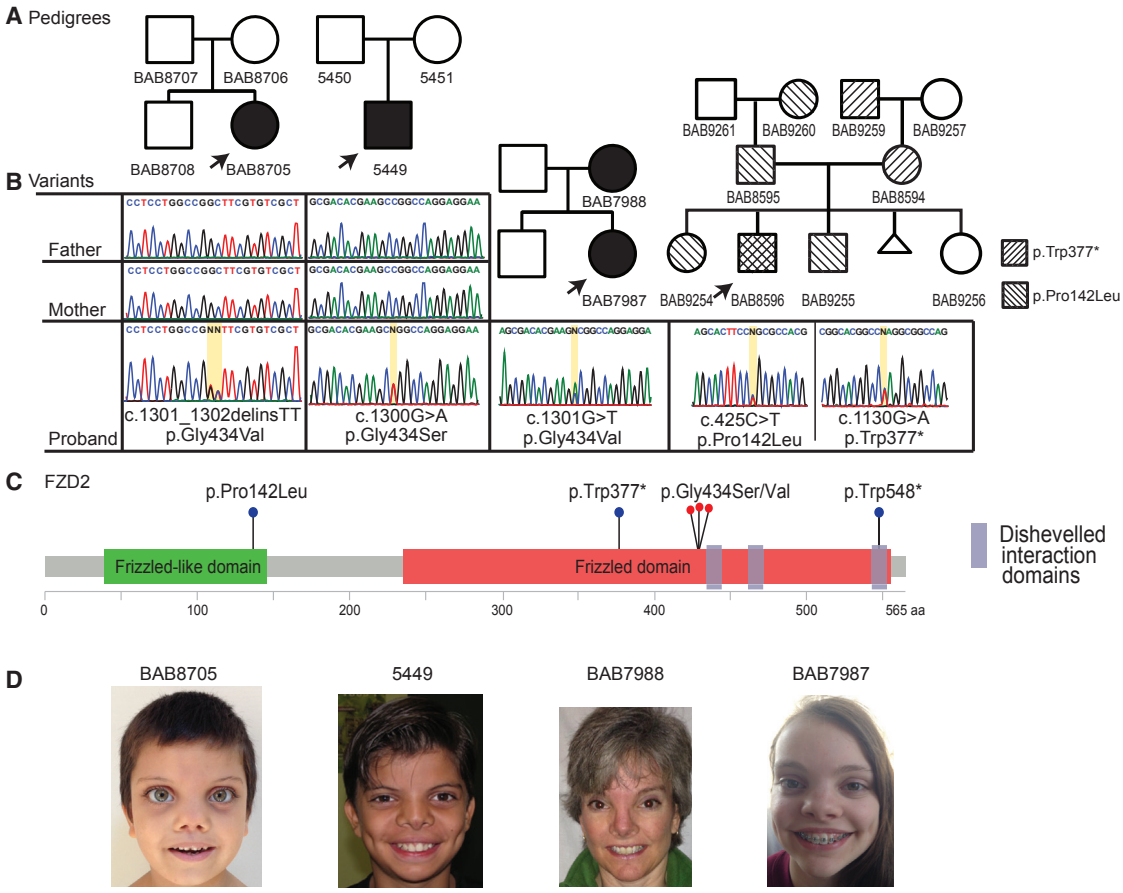

Figure 2. Location of Identified Variants in *FZD2* Segregating with the Associated Phenotypic Features
(A) Pedigrees of the four probands with Robinow syndrome features, carrying variants in *FZD2*.
(B) Sanger sequencing traces for index case subjects, demonstrating the detected variants at the nucleotide level. Family of BAB8596, far right, contains two variants in *FZD2*: p.Trp377* and p.Pro142Leu. The stop gain was inherited from an affected mother and the missense represents a variant of uncertain significance inherited from father.
(C) Representation of the known functional domains of *FZD2* (green and red rectangles).[86] Location of protein-coding variants identified in our cohort: one stop gain and three recurrent variants all affecting glycine 434 located within the third intracellular loop (red dots). One additional variant (p.Trp548*) from the literature, and reported in association with omodysplasia, is also included.[46]
(D) Photographs of consenting subjects with *FZD2* variants demonstrating shared facial characteristics consisting of a high, broad forehead, prominent eyes, broad and low nasal bridge, low-set ears, broad nasal tip, and anteverted nares.

affected mother, BAB8594, who has a milder form of DRS; her phenotype includes short stature, a high and broad forehead, and mesomelia. The proband presents with short stature, RS facial characteristics (more prominent in him than in his mother), and mesomelia early in life that improved with age as assessed both clinically and by radiographic measurement (Figure S3 and Supplemental Note). The VUS was inherited from his father, BAB8595, and is present in two siblings, BAB9254 and BAB9255, all of whom have short stature but no other features consistent with RS (Table 1). Therefore, we are unable to determine the potential genetic contribution of this VUS to the phenotypes observed in this family. An alternative interpretation of the *FZD2* variant data and segregation in this family is that the VUS may be benign and the short stature observed in this pedigree, a result of assortative mating, as both maternal and paternal lineages are significant for short stature with the proband's expected mid-parental height of 162 cm (<2nd centile).

Pertinent clinical information in all individuals with variants in *FZD2* is shown in Table 1 (see Supplemental Note for detailed clinical case reports). The clinical presentation of affected individuals could be considered a constellation of features representing a distinct disorder that includes short stature, limb defects, and shared facial characteristics that includes a high, broad forehead, flat face, low-set ears, broad nasal tip, and anteverted nares (Figure 2D). In addition, all affected individuals (6/6) have mesomelia or micromelia, 4/6 have brachydactyly, and 5/6 have significant short stature. Alternatively, as a result of the broad variable expressivity of associated RS features, individuals with *FZD2* variants could be considered as atypical RS case subjects. In fact, *FZD2* has been proposed in a single family as a candidate gene for omodysplasia[40] (MIM: 258315), a disorder that significantly overlaps with RS. Indeed, the clinical similarities between omodysplasia and DRS are striking. Given the observations that FZD2, WNT5A, and DVL1 and DVL3 interact molecularly and

Table 1. Phenotypic Features of Individuals with *FZD2* (GenBank: NM_001466.3) Variants

Individual ID	5449	BAB8705	BAB7987	BAB7988	BAB8596	BAB8594	BAB9254*	BAB9255*
Zygosity	het	het	het	het	comp het	het	het	het
Variant	c.1300G>A	c.1301_1302delinsTT	c.1301G>T	c.1301G>T	c.1130G>A, c.425C>T	c.1130G>A	c.425C>T	c.425C>T
Effect	p.Gly434Ser	p.Gly434Val	p.Gly434Val	p.Gly434Val	p.Trp377*, p.Pro142Leu	p.Trp377*	p.Pro142Leu	p.Pro142Leu
Age last examination	10 y 3 mo	5 y 8 mo	15 y	47 y	6 y 7 mo	30 y	8 y 4 mo	4 y 3 mo
Inheritance	*de novo*	*de novo*	inherited	unknown; affected mother of BAB7987	inherited	inherited; affected mother of BAB8596	inherited; sister of BAB8596	inherited; brother of BAB8596
Gender	M	F	F	F	M	F	F	M
Growth								
Height SD	45th centile	−2.9 SD	−2.25 SD	−1.7 SD	−3.5 SD	−2.1 SD	−4.5 SD	−2.6 SD
Facial Features								
Macrocephaly	−	relative	−	+	−	−	−	−
Broad forehead	+	+	+	+	+	+	−	−
High forehead	+	+	−	−	+	+	−	−
Midface hypoplasia	+	+	+	+	−	−	−	−
Hypertelorism	+	+	+	+	−	−	−	−
Long eyelashes	mild +	+	+	+	+	−	−	−
Prominent eyes	+	+	+	+	−	−	−	−
Anteverted nares	+	+	+	+	+	+	−	−
Wide nasal bridge	+	+	−	ND	−	−	−	−
Thin vermillion border	+	+	+	+	−	−	−	−
Gingival hyperplasia	+	+	+	+	ND	ND	−	−
Bilobed tongue	−	+	+	+	−	−	−	−
Dental anomalies	+	+	+	+	−	−	−	−
Low set ears	+	+	+	+	+	+	−	−
Skeletal								
Hand length	14.5 cm (−1 SD)	ND	ND	ND	11.5 cm	15.5L 15.7R	12 cm	10 cm
Limbs	mesomelia	micromelia	mesomelia	mesomelia	mesomelia, improved with age	mesomelia	micromelia	micromelia

(*Continued on next page*)

Table 1. *Continued*

Individual ID	5449	BAB8705	BAB7987	BAB7988	BAB8596	BAB8594	BAB9254*	BAB9255*
Brachydactyly	+	+	+	+	–	–	–	–
Clinodactyly	5th fingers +	5th fingers +	+	+	–	–	–	–
Camptodactyly	short low implanted thumbs	4th fingers +	–	–	–	–	–	–
Broad thumb	–	+	–	–	–	–	–	–
Broad 1st toe	–	+	+	+	–	–	–	–
Other Features								
Genital hypoplasia	–	+	+	+	–	ND	–	–
Renal anomalies	–	–	–	+	–	–	–	–
Cardiac anomalies	–	–	–	–	–	–	–	–

Abbreviations: ND, no data; het, heterozygous. Asterisk (*) indicates subjects not diagnosed with Robinow syndrome.

the shared phenotype between omodysplasia and RS, these data are consistent with the hypothesis that omodysplasia represents a subset of RS with predominant short humeri and radial head dislocation collectively representing a point on the spectrum of RS, rather than a distinct clinical syndrome. The characteristic "fetal face" is present in all affected individuals with additional skeletal and limb defects of varying severity but this would not meet a strict clinical diagnostic criterion for DRS, except for BAB7987, BAB7988, and BAB8596. Although there have been previous reports of RS-affected individuals without limb defects, it is unclear whether this cohort of affected individuals would constitute necessary phenotypic overlap to clinically describe this as RS or a distinct disorder of variable severity.[41]

Biallelic Variants in *NXN* Cause Recessive Robinow Syndrome

One individual clinically diagnosed with RS, BAB8841, carries a homozygous stopgain variant in *NXN* (GenBank: NM_022463.4; c.625C>T [p.Arg209*]) inherited from consanguineous parents (Figure 3A). GeneMatcher[37] identified a second family with two affected siblings (BAB9844, BAB9847) who shared compound heterozygous biallelic variants in *NXN*: a maternally inherited in-frame 3-bp deletion (GenBank: NM_022463.4; c.1234_1236del [p.Glu412del]) and a paternally inherited intragenic 84-kb deletion that encompasses the entire first exon: seq[GRCh37]del (17)(p13.3) chr17:g.805043::GAGG…..AATG::889090) (Figures 3A, 3B, and S4). Deletion CNVs can often account for disease-associated pathogenic alleles at both AD and AR disease trait loci.[42–44] This specific *NXN* exon 1 deletion CNV is mediated by two directly orientated *Alu* elements (*AluSx-AluSx1*) sharing 81% nucleotide identity (Figure 3B); such *Alu-Alu*-mediated exonic deletions often involve different *Alu* family members located within flanking introns. Remarkably, *NXN* maps to 17p13.3, which has a high *Alu* density and likely elevated rates of *Alu-Alu*-mediated rearrangements,[45] indicating that future diagnostic efforts should include copy-number analyses for this locus. The first and last exons of a multi-exon gene may be particularly prone to *Alu-Alu*-mediated deletion CNVs related to the abundance of *Alu* elements flanking the 5′ and 3′ ends of the gene which can be used as template switch substrates during microhomology-mediated break-induced replicative repair.[46,47]

NXN encodes an oxidative stress response protein, nucleoredoxin, which is highly expressed in the developing limb bud of mice.[48] Abnormal activation of the Wnt/β-catenin signaling in $Nxn^{-/-}$ knockout mice is hypothesized to lead to the observed craniofacial defects, a phenotype perhaps relevant to the subjects with RRS reported herein due to biallelic *NXN* variants that are likely loss-of-function alleles. Moreover, studies in *Xenopus laevis* have collectively shown that Nxn acts as

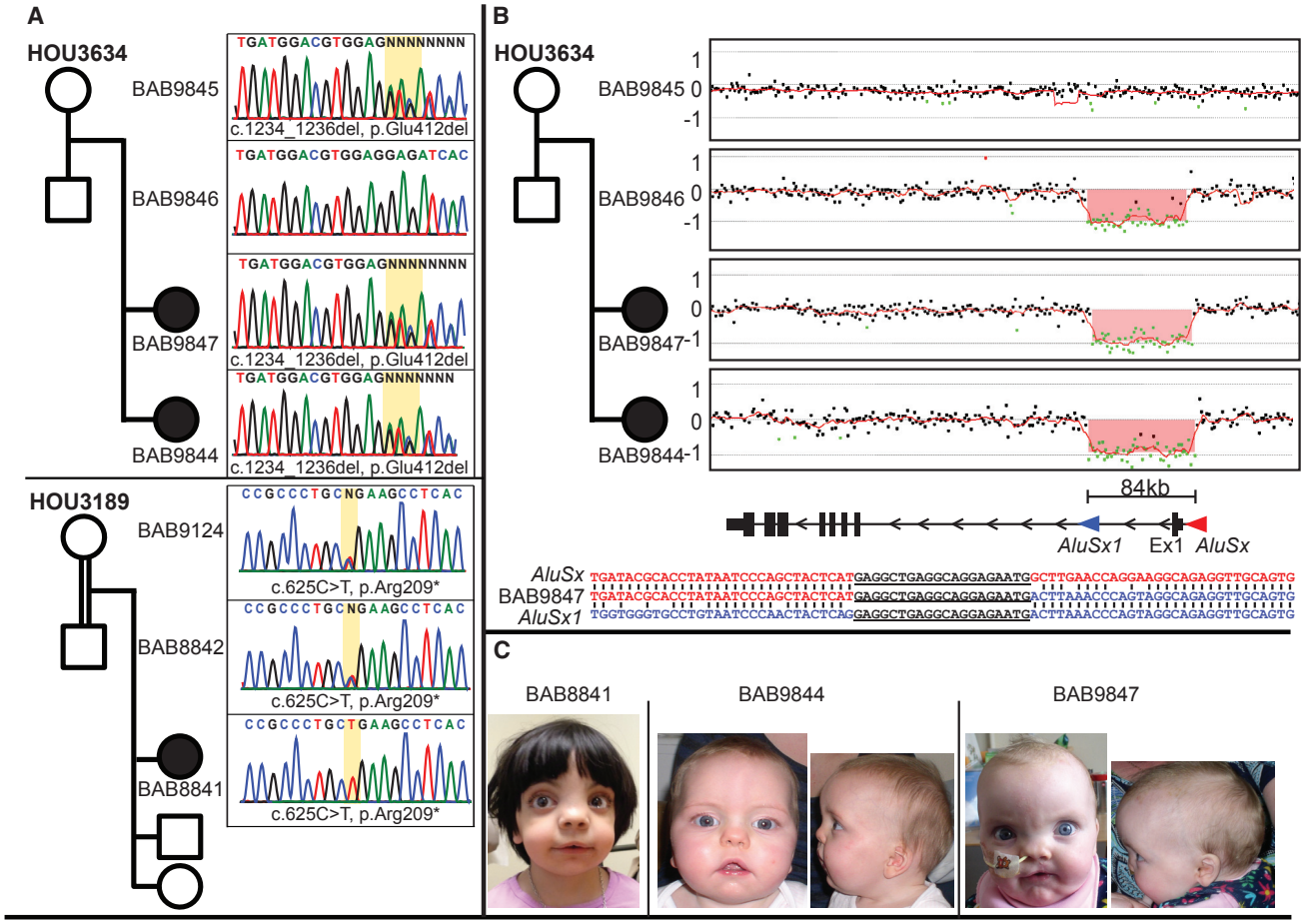

Figure 3. Identified Biallelic Variants in *NXN*

(A) Pedigrees and Sanger sequencing traces for the two families with variants in *NXN*; a homozygous stop gain in BAB8841 (family HOU3189) and a heterozygous 3-bp in-frame deletion in BAB9847 and BAB9844 (family HOU3634).

(B) High-density arrays and breakpoint mapping showing the second mutant allele in BAB9847 and BAB9844. The deletion is mediated by two highly similar *Alu* elements in direct orientation that flank the first coding exon.

(C) Facial pictures demonstrating shared facial features including high forehead, prominent eyes, broad and low nasal bridge, broad nasal tip, anteverted nares, and micrognathia.

a negative regulator of the Wnt/PCP pathway potentially by blocking the ubiquitination and degradation of Dvl as well as inhibiting Dvl-induced c-*jun* phosphorylation via Rac, the crucial biochemical mechanism underlying the Wnt/PCP pathway.[19,20] Two independent *Nxn*$^{-/-}$ mouse models show abnormal craniofacial morphology with a shortened snout and cleft palate partially recapitulating the RS subjects' phenotype.[49,50] The individuals with biallelic variants in *NXN* present with a phenotype consistent with a diagnosis of RS, wherein all three identified individuals have typical facial characteristics, mesomelia, brachydactyly, and broad thumbs/toes (Figure 3C and Supplemental Note for detailed clinical case reports).[51]

Identification of Additional Robinow Syndrome Candidate Disease-Associated Genes

In two affected individuals we identified likely pathogenic rare variants in association with the rare RS phenotype in two distinct candidate genes whose function has been demonstrated to play an important role in Wnt/PCP signaling: *RAC3* and *GPC4*. These include one sporadic Robinow-like individual (BAB8740) with a *de novo* missense variant in *RAC3* (GenBank: NM_005052.2; c.176C>G [p.Ala59Gly]). Another individual (BAB8295) has a hemizygous nonsynonymous missense variant in *GPC4* (GenBank: NM_001448.2; c.1235G>A [p.Arg412Lys]) inherited from a heterozygous unaffected mother, potentially responsible for an X-linked form of RS. We propose *RAC3* and *GPC4* to be candidate genes underlying Robinow-like features due to the shared interactome and signaling network of known (*WNT5A*, *ROR2*, *DVL1*, *DVL3*) and currently described (*FZD2*, *NXN*) RS disease-relevant genes. In addition, both affected subjects share the same rare phenotype and the exceedingly rare nature of the mutant alleles. *RAC3* is a member of the Rac subfamily of the Rho family of GTPases, which specifically interacts with DVL in response to Wnt ligand to activate downstream effects including JNK/c-*jun* phosphorylation essential for cytoskeletal reorganization.[52] *GPC4* is one of the six members of the heparin sulfate proteoglycans, which are key players in

endochondral ossification[53] with defects in *GPC6* (MIM: 604404) and *GPC3* (MIM: 300037) resulting in the skeletal disorders omodysplasia[54] and Simpson-Golabi-Behmel syndrome (MIM: 312870),[55] respectively. Specifically, *GPC4* has been shown to be a positive regulator of Wnt/PCP signaling by promoting the accumulation of dishevelled at the cell membrane[56] and can rescue *Drosophila* Dfz2 aberrant Wnt signaling phenotypes.[57] Indeed, duplications of *GPC4* have been associated with Simpson-Golabi-Behmel syndrome;[58] however, loss of *gpc4* in *Danio rerio* results in dwarfism phenotypes, which may represent an unspecific finding.[59] The clinical phenotype of individuals harboring candidate variants is consistent with earlier clinical descriptions of DRS with varying severity of associated traits;[51] shared phenotypes are shown in Table 2 (see Supplemental Note for detailed clinical descriptions).

Discussion

The concept that mutation in distinct genes could lead to the same phenotype was first suggested almost a century ago by William Allan when he observed multiple modes of inheritance (AD, AR, XL) for Charcot-Marie-Tooth disease consistent with at least two genetic loci (autosomal and X-linked);[60] this was further demonstrated by N.E. Morton more than 60 years ago, wherein elliptocytosis was mathematically linked to two distinct human loci in different families.[61] Although genetic heterogeneity has been known for some time, only recently with comprehensive clinical phenotyping, syndrome characterization, and cataloguing of Mendelian disease traits through the efforts of OMIM can we begin to appreciate the frequency of genetic heterogeneity.[62] As of April 2017, an estimated 12.5% (395/4,931) of Mendelian phenotypes have had disease-causing mutations identified in two or more genes represented as a "phenotypic series."[63] Genetic heterogeneity can be viewed as an obstacle to identifying disease-gene associations, although it is also recognized that overlapping phenotypes arising from distinct loci might reflect perturbed protein interactions or shared biological relationships.[64] Accordingly, genetically heterogeneous disorders provide an opportunity for insight into the pathways and biological underpinnings of disease, wherein a single syndrome provides evidence for the aberrant interactome, network, or biological signaling cascade.

Noncanonical Wnt signaling regulates, via the PCP pathway, convergent extension movements, an essential cell migration process during vertebrate gastrulation.[65] The aforementioned developmental processes in different organisms are largely controlled by the same set of core PCP proteins, which were originally identified in *Drosophila*. However, compared to *Drosophila,* the vertebrate PCP pathway has evolved and diversified by specification and emergence of multiple paralogs from a single fly gene, throughout nearly all of the core components of this pathway. Not surprisingly, recent studies have demonstrated that genes that are essential in flies and have multiple human orthologs are more likely to be associated with human disease than are fly genes with a single human ortholog,[10] potentially indicating duplication and further paralog specialization during evolution from flies to human. Indeed, in vertebrates, Wnt/PCP signaling partially drives the patterning and formation of the limb-bud outgrowth and growth plate in skeletal formation.[66,67] Of particular interest is the organized cellular division and planar alignment of proliferating chondrocytes at the growth plate, as this process is dependent on Wnt/PCP activation and defects result in abnormal growth plate chondrocyte localization and morphology with skeletal defects analogous to RS.[66,68,69]

Genetic screening in *Drosophila* identified many of the components of the PCP pathway including both frizzled[70] and dishevelled.[71] We provide evidence that variants in multiple WNT/PCP signaling genes can be associated with RS including *FZD2* and *NXN* in autosomal-dominant and -recessive inheritance patterns, respectively. *FZD2* encodes the highly conserved seven-pass transmembrane protein of the Frizzled family of membrane receptors. Frizzled was originally identified by Vinson and Adler in *Drosophila melanogaster* with "clinical findings" of misoriented cuticle hairs, which they named *frizzled*.[70] Interestingly, similar to all other Robinow-associated proteins, FZD2 is implicated in the Wnt/PCP pathway, in which studies have demonstrated Frizzled proteins functioning as Wnt receptors and co-receptors[72,73] and is required for the WNT5A-mediated recruitment of DVL2 (MIM: 602151) to the membrane.[74] WNT5A binding, in the presence of ROR1 (MIM: 602336), ROR2, and DVL2, induces clathrin-mediated internalization of FZD2, which is necessary for RAC1 activation in HEK293 cells.[74]

NXN demonstrates a specific redox-dependent interaction with dishevelled via the PDZ domain; in fact, pull-down assays of mouse fibroblasts indicate that NXN is a substantial interacting partner of DVL1, particularly under oxidative conditions,[20] often stimulated by growth factors.[75] *In vitro* association with DVL2 and DVL3 has also been demonstrated.[76] The interaction of NXN and DVL may be a key regulatory mechanism to maintain a spatial or temporal balance between canonical and noncanonical Wnt pathways during development. Evidence for this includes the fact that NXN specifically inhibits DVL function *in vitro* whereas it also blocks ubiquitination and degradation of DVL via KLHL12 in a tissue-specific manner; the latter helps to regulate transmission of Wnt/β-catenin signal upon Wnt stimulation.[20,49] In addition, tissue-specific dysregulation of Wnt/β-catenin signaling was experimentally demonstrated in $Nxn^{-/-}$ mice in which osteoblastic cells show excessive differentiation associated with strong Wnt/β-catenin signaling activation compared to osteoblasts of $Nxn^{+/+}$ mice whereas mouse embryonic fibroblast cells show impaired Wnt/β-catenin signaling.[49] Collectively, there is ample evidence in the literature that disruption of Frizzled and

Table 2. Phenotypic Features of Individuals with Variants in RS Candidate Genes *NXN* (Recessive), *RAC3* (Dominant), and *GPC4* (X-Linked)

Individual ID	BAB8841	BAB9847	BAB9844	BAB8740	BAB8295
Gene	*NXN*	*NXN*	*NXN*	*RAC3*	*GPC4*
GenBank	NM_022463.4	NM_022463.4	NM_022463.4	NM_005052.2	NM_001448.2
Zygosity	hom	comp het	comp het	het	hemizygous
Variant(s)	c.625C>T	c.1234_1236del	c.1234_1236del	c.176C>G	c.1235G>A
		chr17:g.805043::GAGG….AATG::889090	chr17:g.805043::GAGG….AATG::889090		
Effect	p.Arg209*	p.Glu412del, ?	p.Glu412del, ?	p.Ala59Gly	p.Arg412Lys
Consanguinity	+	−	−	−	−
Age last examination	5 y	2 y 5 mo	4 wk	13 y 2 mo	8 y
Inheritance	inherited	inherited	inherited	*de novo*	inherited
Gender	F	F	F	F	M
Facial Features					
Macrocephaly	+	relative	relative	−	+
Frontal bossing	−	+	+	−	+
High forehead	+	+	+	−	+
Midface hypoplasia	−	+	+	+	+
Hypertelorism	+	+	+	+	+
Long eyelashes	+	−	−	+	−
Prominent eyes	+	+	+	+	−
Anteverted nares	+	+	+	+	+
Wide nasal bridge	−	+	+	+	+
Short nose	−	+	+	+	−
Long philtrum	+	+	+	+	−
Triangular mouth	+	+	+	−	+
Gingival hyperplasia	+	+	+	−	+
Absent uvula	+	−	+	−	−
Cleft soft palate	−	−	+	−	+
Dental anomalies	+	−	ND	+	delayed dental eruption
Micrognathia	+	+	+	+	−

(*Continued on next page*)

Table 2. *Continued*

Individual ID	BAB8841	BAB9847	BAB9844	BAB8740	BAB8295
Skeletal					
Mesomelia	+	+ improved with age	+	–	+
Brachydactyly	+	+	+	–	+
Clinodactyly	+	+	+	+	+
Camptodactyly	–	+	+	–	+
Broad thumb	+	+	+	–	+
Fetal finger/toe pads	–	+	+	+	–
Broad 1st toe	+	+	+	–	+
Other Features					
Genital hypoplasia	ND	–	–	+	–
Renal anomalies	+	–	–	–	–
Cardiac anomalies	+	–	–	–	PDA

Abbreviations: ND, no data; hom, homozygous; het, heterozygous; PDA, patent ductus arteriosus.

noncanonical Wnt signaling leads to delay or block in chondrocyte maturation and shortening of skeletal elements,[67,76] which could be the basis of short stature and mesomelia in individuals with RS. Pathogenic variants found in individuals with RS provide insights into the underlying biology of the disease, e.g., loss-of-function mutations affecting the WNT5A receptor ROR2 in ~80% of individuals with RRS[3,4] and hypomorphic mutations affecting WNT5A in ~9.5% of individuals with DRS[6] (Figure 4A), suggesting that the Wnt/PCP pathway is affected in those subjects. This hypothesis is strengthened with the discovery that recurrent truncating variants in both *DVL1* and *DVL3*, leading to C-terminal replacement of those proteins with a highly basic tail, is currently the major cause (33%) of DRS. Furthermore, it has been demonstrated that a subset of *DVL1*-mediated DRS-affected subjects present with osteosclerosis, a phenotype that is associated with perturbed Wnt signaling.[8] Such mutational specificity in both *DVL1* and *DVL3* is intriguing and suggest a specific role in the noncanonical pathway. Despite DVL being an important contributor in diverse signaling pathways,[11] its C terminus is characterized by (1) having a conserved DEP domain that works in the PCP signaling, (2) being required for membrane recruitment via Wnt-mediated signaling,[77] (3) carrying relevant phosphorylation sites that specify DVL functions and subcellular localization,[78,79] and (4) being necessary to establish and to stabilize protein-protein interactions with ROR2[12] as well as FZD2.[38] In fact, our current study indicates that variants affecting *FZD2* specifically lead to DRS or Robinow-like traits[40] when all the DVL interaction domains either are removed (p.Trp377*) or are adjacent to them (p.Gly434Ser/Val) (Figure 2C). Moreover, *NXN*, a gene that encodes a redox-dependent regulator of DVL, was identified in 5% (one family) of this clinically ascertained RS cohort and appears to cause a new recessive form of RS. Compound heterozygous variants within this gene co-segregating with the disease were further observed in another family, confirming our initial observation. *NXN* is a potent regulator of DVL stability, particularly in conditions of high oxidative stress,[49] circumstances intriguingly similar to the high levels of reactive oxygen species during chondrocyte hypertrophy at the growth plate.[80] The relevance of *NXN* mutations for RRS requires further studies in other unsolved RS cases.

In aggregate, our data provide supportive experimental evidence that the clinical phenotype in RS results from subtle dysregulation of the Wnt/PCP pathway, contextually affecting the organized proliferation of chondrocytes at the growth plate. A delicate balance between canonical and PCP signaling requires precise regulation of DVL, so it appears that the pathogenesis of Robinow is not simply loss of Wnt/PCP signaling, but a context-specific perturbation in the Wnt signaling. These new findings also support the hypothesis that additional proteins underlying RS or overlapping genetic syndromes will also have a

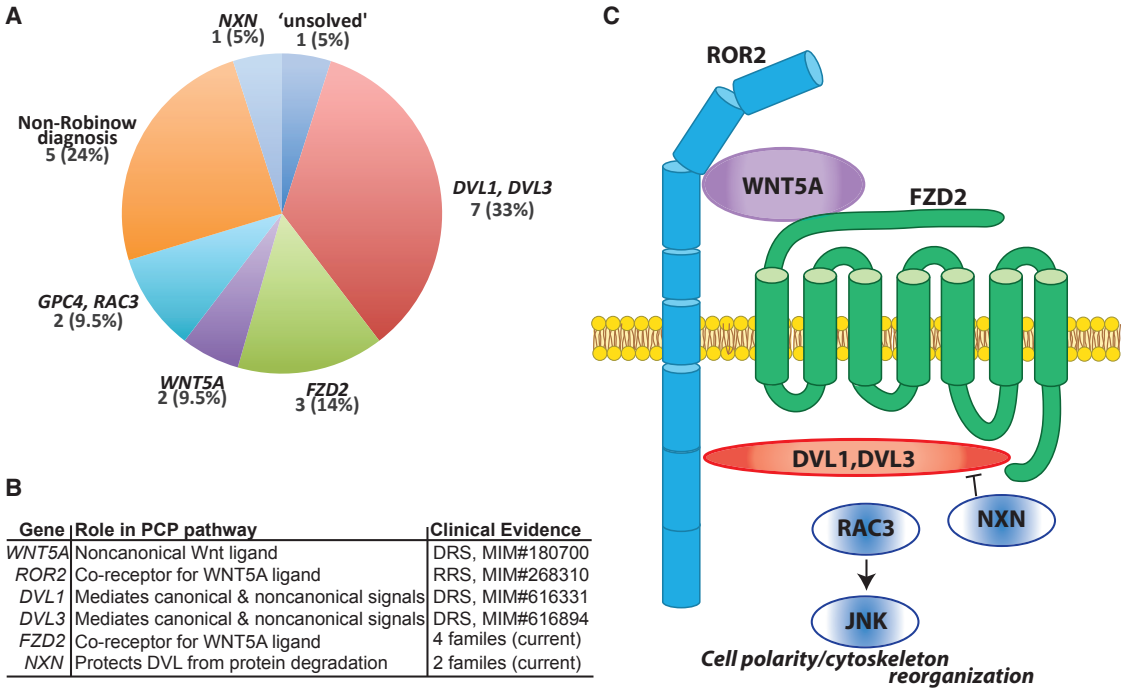

B

Gene	Role in PCP pathway	Clinical Evidence
WNT5A	Noncanonical Wnt ligand	DRS, MIM#180700
ROR2	Co-receptor for WNT5A ligand	RRS, MIM#268310
DVL1	Mediates canonical & noncanonical signals	DRS, MIM#616331
DVL3	Mediates canonical & noncanonical signals	DRS, MIM#616894
FZD2	Co-receptor for WNT5A ligand	4 familes (current)
NXN	Protects DVL from protein degradation	2 familes (current)

Figure 4. Robinow Syndrome-Associated Genes in the Wnt/PCP Pathway Identified in Human Subjects
(A) Molecular diagnosis pie chart from the cohort of 21 Robinow syndrome-affected individuals who had a combination of direct Sanger screening and whole-exome sequencing to identify the molecular cause of their disorder highlighting the contribution of *DVL1*, *DVL3*, and *FZD2* variants to RS.
(B and C) The establishment of planar cell polarity is vital for vertebrate development; in humans, variants affecting genes in that pathway are linked to skeletal defects, including Robinow syndrome. *In vitro* studies from several model organisms have demonstrated that ROR2 binds to WNT5A and acts as a co-receptor with FZD2.[5] The downstream effect is routed by the dishevelled homologs, which are stabilized by NXN in a context-dependent manner.[49] The downstream readouts, which ultimately involves cytoskeletal reorganization, are a combination of small GTPases including RAC to activate JNK signaling.[52] Pathogenic variants in all of the aforementioned genes have been identified in individuals with Robinow syndrome, underscoring the notion that this disorder results from aberrant Wnt/PCP signaling, likely due to disturbance of the organized development of chondrocytes at the growth plate.

relevant role in this pathway (Figure 4B). Our data initially indicated that 3 of the 21 families from the RS-affected case subjects remained "unsolved" or without a plausible molecular diagnosis (Figure 4A). However, two of the three unsolved probands in our RS cohort have variants affecting genes biologically relevant in the context of Wnt signaling: a *de novo* mutation in an autosomal gene (*RAC3*) and an X-linked variant in a male from a heterozygous, unaffected mother (*GPC4*). Both genes *RAC3* and *GPC4* are established components of the Wnt/PCP pathway and therefore represent candidate genes that need to be confirmed by the ascertainment of additional affected individuals. In aggregate, personal genome analyses provide a plausible molecular diagnosis that parsimoniously explains the observed clinical phenotype in 95% of individuals clinically diagnosed with Robinow; i.e., 20/21 subjects investigated.

In summary, we demonstrate that the study of rare human syndromes and phenotypes can provide insight into human biology, a Garrodian principle stemming from the early pioneers of human genetics.[1,81] Figure 4C depicts a representative model for the physical interactions of all identified Robinow-associated proteins with a role in the Wnt/PCP pathway that have been identified in human mutational studies thus far. Of note, in this cohort all variant types—single-nucleotide variants (SNVs), indels, and copy-number variants (CNVs)—were found to be pathogenic and a multitude of mutational processes, including *Alu-Alu*-mediated rearrangement resulting in exonic deletion[82,83] and secondary structure mutagenesis for recurrent indel formation,[84] were shown to be operative. In dissecting the etiology of non-allelic genetic heterogeneity in RS, we observe strong evidence that disturbed levels of a complex interplay of noncanonical and canonical Wnt signaling underlies the core phenotype exhibited by affected individuals. The relevance of this observation becomes clear when considering that canonical and noncanonical pathways use common intracellular components and that specificity of distinct Wnt signaling pathways is regulated by the combination of ligands and receptors in a particular cellular context. In this way, the same proteins in distinct cellular environments may inhibit or trigger a given signal branch. For example, FZD2 can either inhibit or trigger canonical and non-canonical β-catenin pathways depending on the presence of additional transmembrane receptors.[74] Ligation of WNT5A to FZD2 was shown to inhibit canonical β-catenin in addition to activate the noncanonical pathway in HEK293 cells, as measured by downstream RAC1 activation, the latter depending on the presence of ROR1, ROR2, and

DVL2. The discovery of the main gene contributors in RS will likely further clarify underlying molecular mechanism in other skeletal dysplasias with an overlapping phenotype, as for example, in omodysplasia.

As we progress in our molecular and genetic understanding of many Mendelian disease traits, it is important to understand and appreciate genetic heterogeneity, clinical variability, and overlap of clinical features (i.e., phenotypic signs/symptoms) with other disorders. Here we have approached gene discovery in a phenotype-driven manner, using an unbiased genomics rather than locus-specific approach, i.e., a Mendelian genomics versus Mendelian genetics single-gene/locus approach. As shown here, Mendelian genomics can readily investigate the underpinnings of genetic heterogeneity of disease traits as well as explore mutational burden and multi-locus variation models for disease.[33,85] This study has enabled the identification of pathway-specific candidate disease-associated genes in RS, the specific paralogs involved, assessed the contribution of known genes, and provided insights into underlying mechanisms of a disease marked by genetic heterogeneity, which ultimately revealed the contribution of key proteins to limb formation and human development.

Accession Numbers

The accession numbers for identified variants were deposited into ClinVar with the following identifiers: SCV000583563–SCV000583582.

Supplemental Data

Supplemental Data include four figures, two tables, and Supplemental Notes of case reports and can be found with this article online at https://doi.org/10.1016/j.ajhg.2017.10.002.

Conflicts of Interest

J.R.L. has stock ownership in 23andMe, is a paid consultant for Regeneron Pharmaceuticals, has stock options in Lasergen, Inc., and is a co-inventor on multiple United States and European patents related to molecular diagnostics for inherited neuropathies, eye diseases, and bacterial genomic fingerprinting. The Department of Molecular and Human Genetics at Baylor College of Medicine derives revenue from molecular genetic testing offered in the Baylor-Genetics Laboratories.

Acknowledgments

The authors would like to thank the individuals and their families who contributed to this study and the Robinow Syndrome Foundation for facilitating collaboration. Supported by the US National Human Genome Research Institute/National Heart Blood Lung Institute jointly funded Baylor Hopkins Center for Mendelian Genomics (UM1 HG006542). J.J.W. was funded in part by the Smith-Magenis Syndrome Research Foundation (SMSRF). A.M.V.-M. is funded by FAPESP (CEPID 2013/08028-1). The content is solely the responsibility of the authors and does not necessarily represent the official views of the NHGRI/NHBLI, NIH.

Received: May 26, 2017
Accepted: October 6, 2017
Published: December 21, 2017

Web Resources

1000 Genomes, http://www.internationalgenome.org/
Atherosclerosis Risk in Communities Study (ARIC) Database, http://www2.cscc.unc.edu/aric/
Baylor Genetics Laboratory, http://bmgl.com/
BCM HGSC Mercury, https://www.hgsc.bcm.edu/software/mercury
ClinVar, https://www.ncbi.nlm.nih.gov/clinvar/
dbGaP, http://www.ncbi.nlm.nih.gov/gap
ExAC Browser, http://exac.broadinstitute.org/
GenBank, https://www.ncbi.nlm.nih.gov/genbank/
OMIM, http://www.omim.org/
RefSeq, http://www.ncbi.nlm.nih.gov/RefSeq
Robinow Syndrome Foundation, http://www.Robinow.org

References

1. Garrod, A. (1928). The lessons of rare maladies: annual oration before the medical society of London by Sir Archibald Garrod. BMJ *1*, 914–915.
2. Robinow, M., Silverman, F.N., and Smith, H.D. (1969). A newly recognized dwarfing syndrome. Am. J. Dis. Child. *117*, 645–651.
3. van Bokhoven, H., Celli, J., Kayserili, H., van Beusekom, E., Balci, S., Brussel, W., Skovby, F., Kerr, B., Percin, E.F., Akarsu, N., and Brunner, H.G. (2000). Mutation of the gene encoding the ROR2 tyrosine kinase causes autosomal recessive Robinow syndrome. Nat. Genet. *25*, 423–426.
4. Afzal, A.R., Rajab, A., Fenske, C.D., Oldridge, M., Elanko, N., Ternes-Pereira, E., Tüysüz, B., Murday, V.A., Patton, M.A., Wilkie, A.O., and Jeffery, S. (2000). Recessive Robinow syndrome, allelic to dominant brachydactyly type B, is caused by mutation of ROR2. Nat. Genet. *25*, 419–422.
5. Oishi, I., Suzuki, H., Onishi, N., Takada, R., Kani, S., Ohkawara, B., Koshida, I., Suzuki, K., Yamada, G., Schwabe, G.C., et al. (2003). The receptor tyrosine kinase Ror2 is involved in non-canonical Wnt5a/JNK signalling pathway. Genes Cells *8*, 645–654.
6. Person, A.D., Beiraghi, S., Sieben, C.M., Hermanson, S., Neumann, A.N., Robu, M.E., Schleiffarth, J.R., Billington, C.J., Jr., van Bokhoven, H., Hoogeboom, J.M., et al. (2010). WNT5A mutations in patients with autosomal dominant Robinow syndrome. Dev. Dyn. *239*, 327–337.
7. White, J., Mazzeu, J.F., Hoischen, A., Jhangiani, S.N., Gambin, T., Alcino, M.C., Penney, S., Saraiva, J.M., Hove, H., Skovby, F., et al.; Baylor-Hopkins Center for Mendelian Genomics (2015). *DVL1* frameshift mutations clustering in the penultimate exon cause autosomal-dominant Robinow syndrome. Am. J. Hum. Genet. *96*, 612–622.
8. Bunn, K.J., Daniel, P., Rösken, H.S., O'Neill, A.C., Cameron-Christie, S.R., Morgan, T., Brunner, H.G., Lai, A., Kunst, H.P., Markie, D.M., and Robertson, S.P. (2015). Mutations in

DVL1 cause an osteosclerotic form of Robinow syndrome. Am. J. Hum. Genet. *96*, 623–630.
9. White, J.J., Mazzeu, J.F., Hoischen, A., Bayram, Y., Withers, M., Gezdirici, A., Kimonis, V., Steehouwer, M., Jhangiani, S.N., Muzny, D.M., et al.; Baylor-Hopkins Center for Mendelian Genomics (2016). *DVL3* alleles resulting in a -1 frameshift of the last exon mediate autosomal-dominant Robinow syndrome. Am. J. Hum. Genet. *98*, 553–561.
10. Yamamoto, S., Jaiswal, M., Charng, W.-L., Gambin, T., Karaca, E., Mirzaa, G., Wiszniewski, W., Sandoval, H., Haelterman, N.A., Xiong, B., et al. (2014). A Drosophila genetic resource of mutants to study mechanisms underlying human genetic diseases. Cell *159*, 200–214.
11. Gao, C., and Chen, Y.G. (2010). Dishevelled: The hub of Wnt signaling. Cell. Signal. *22*, 717–727.
12. Witte, F., Bernatik, O., Kirchner, K., Masek, J., Mahl, A., Krejci, P., Mundlos, S., Schambony, A., Bryja, V., and Stricker, S. (2010). Negative regulation of Wnt signaling mediated by CK1-phosphorylated Dishevelled via Ror2. FASEB J. *24*, 2417–2426.
13. Mlodzik, M. (2002). Planar cell polarization: do the same mechanisms regulate Drosophila tissue polarity and vertebrate gastrulation? Trends Genet. *18*, 564–571.
14. Strutt, H., Warrington, S.J., and Strutt, D. (2011). Dynamics of core planar polarity protein turnover and stable assembly into discrete membrane subdomains. Dev. Cell *20*, 511–525.
15. Lei, Y.-P., Zhang, T., Li, H., Wu, B.-L., Jin, L., and Wang, H.-Y. (2010). VANGL2 mutations in human cranial neural-tube defects. N. Engl. J. Med. *362*, 2232–2235.
16. Allache, R., De Marco, P., Merello, E., Capra, V., and Kibar, Z. (2012). Role of the planar cell polarity gene *CELSR1* in neural tube defects and caudal agenesis. Birth Defects Res. Part A - Clin. Mol. Teratol. *94*, 176–181.
17. Torban, E., Patenaude, A.-M., Leclerc, S., Rakowiecki, S., Gauthier, S., Andelfinger, G., Epstein, D.J., and Gros, P. (2008). Genetic interaction between members of the Vangl family causes neural tube defects in mice. Proc. Natl. Acad. Sci. USA *105*, 3449–3454.
18. Robinson, A., Escuin, S., Doudney, K., Vekemans, M., Stevenson, R.E., Greene, N.D., Copp, A.J., and Stanier, P. (2012). Mutations in the planar cell polarity genes *CELSR1* and SCRIB are associated with the severe neural tube defect craniorachischisis. Hum. Mutat. *33*, 440–447.
19. Funato, Y., Michiue, T., Terabayashi, T., Yukita, A., Danno, H., Asashima, M., and Miki, H. (2008). Nucleoredoxin regulates the Wnt/planar cell polarity pathway in Xenopus. Genes Cells *13*, 965–975.
20. Funato, Y., Michiue, T., Asashima, M., and Miki, H. (2006). The thioredoxin-related redox-regulating protein nucleoredoxin inhibits Wnt-beta-catenin signalling through dishevelled. Nat. Cell Biol. *8*, 501–508.
21. Chong, J.X., Buckingham, K.J., Jhangiani, S.N., Boehm, C., Sobreira, N., Smith, J.D., Harrell, T.M., McMillin, M.J., Wiszniewski, W., Gambin, T., et al.; Centers for Mendelian Genomics (2015). The genetic basis of Mendelian phenotypes: discoveries, challenges, and opportunities. Am. J. Hum. Genet. *97*, 199–215.
22. Bainbridge, M.N., Wang, M., Wu, Y., Newsham, I., Muzny, D.M., Jefferies, J.L., Albert, T.J., Burgess, D.L., and Gibbs, R.A. (2011). Targeted enrichment beyond the consensus coding DNA sequence exome reveals exons with higher variant densities. Genome Biol. *12*, R68.
23. McCarthy, D.J., Humburg, P., Kanapin, A., Rivas, M.A., Gaulton, K., Cazier, J.B., and Donnelly, P. (2014). Choice of transcripts and software has a large effect on variant annotation. Genome Med. *6*, 26.
24. Reid, J.G., Carroll, A., Veeraraghavan, N., Dahdouli, M., Sundquist, A., English, A., Bainbridge, M., White, S., Salerno, W., Buhay, C., et al. (2014). Launching genomics into the cloud: deployment of Mercury, a next generation sequence analysis pipeline. BMC Bioinformatics *15*, 30.
25. Eldomery, M.K., Coban-Akdemir, Z., Harel, T., Rosenfeld, J.A., Gambin, T., Stray-Pedersen, A., Küry, S., Mercier, S., Lessel, D., Denecke, J., et al. (2017). Lessons learned from additional research analyses of unsolved clinical exome cases. Genome Med. *9*, 26.
26. Fromer, M., Moran, J.L., Chambert, K., Banks, E., Bergen, S.E., Ruderfer, D.M., Handsaker, R.E., McCarroll, S.A., O'Donovan, M.C., Owen, M.J., et al. (2012). Discovery and statistical genotyping of copy-number variation from whole-exome sequencing depth. Am. J. Hum. Genet. *91*, 597–607.
27. Gambin, T., Akdemir, Z.C., Yuan, B., Gu, S., Chiang, T., Carvalho, C.M.B., Shaw, C., Jhangiani, S., Boone, P.M., Eldomery, M.K., et al. (2017). Homozygous and hemizygous CNV detection from exome sequencing data in a Mendelian disease cohort. Nucleic Acids Res. *45*, 1633–1648.
28. Krawczak, M., and Cooper, D.N. (1991). Gene deletions causing human genetic disease: mechanisms of mutagenesis and the role of the local DNA sequence environment. Hum. Genet. *86*, 425–441.
29. Roifman, M., Marcelis, C.L.M., Paton, T., Marshall, C., Silver, R., Lohr, J.L., Yntema, H.G., Venselaar, H., Kayserili, H., van Bon, B., et al.; FORGE Canada Consortium (2015). De novo WNT5A-associated autosomal dominant Robinow syndrome suggests specificity of genotype and phenotype. Clin. Genet. *87*, 34–41.
30. Digilio, M.C., Conti, E., Sarkozy, A., Mingarelli, R., Dottorini, T., Marino, B., Pizzuti, A., and Dallapiccola, B. (2002). Grouping of multiple-lentigines/LEOPARD and Noonan syndromes on the *PTPN11* gene. Am. J. Hum. Genet. *71*, 389–394.
31. Iqbal, Z., Cejudo-Martin, P., de Brouwer, A., van der Zwaag, B., Ruiz-Lozano, P., Scimia, M.C., Lindsey, J.D., Weinreb, R., Albrecht, B., Megarbane, A., et al. (2010). Disruption of the podosome adaptor protein TKS4 (SH3PXD2B) causes the skeletal dysplasia, eye, and cardiac abnormalities of Frank-Ter Haar Syndrome. Am. J. Hum. Genet. *86*, 254–261.
32. Below, J.E., Earl, D.L., Shively, K.M., McMillin, M.J., Smith, J.D., Turner, E.H., Stephan, M.J., Al-Gazali, L.I., Hertecant, J.L., Chitayat, D., et al.; University of Washington Center for Mendelian Genomics (2013). Whole-genome analysis reveals that mutations in inositol polyphosphate phosphatase-like 1 cause opsismodysplasia. Am. J. Hum. Genet. *92*, 137–143.
33. Posey, J.E., Harel, T., Liu, P., Rosenfeld, J.A., James, R.A., Coban Akdemir, Z.H., Walkiewicz, M., Bi, W., Xiao, R., Ding, Y., et al. (2017). Resolution of disease phenotypes resulting from multilocus genomic variation. N. Engl. J. Med. *376*, 21–31.
34. Farwell, K.D., Shahmirzadi, L., El-Khechen, D., Powis, Z., Chao, E.C., Tippin Davis, B., Baxter, R.M., Zeng, W., Mroske, C., Parra, M.C., et al. (2015). Enhanced utility of family-centered diagnostic exome sequencing with inheritance model-based analysis: results from 500 unselected families with undiagnosed genetic conditions. Genet. Med. *17*, 578–586.

35. Yang, Y., Muzny, D.M., Reid, J.G., Bainbridge, M.N., Willis, A., Ward, P.A., Braxton, A., Beuten, J., Xia, F., Niu, Z., et al. (2013). Clinical whole-exome sequencing for the diagnosis of mendelian disorders. N. Engl. J. Med. *369*, 1502–1511.
36. Yang, Y., Muzny, D.M., Xia, F., Niu, Z., Person, R., Ding, Y., Ward, P., Braxton, A., Wang, M., Buhay, C., et al. (2014). Molecular findings among patients referred for clinical whole-exome sequencing. JAMA *312*, 1870–1879.
37. Sobreira, N., Schiettecatte, F., Valle, D., and Hamosh, A. (2015). GeneMatcher: a matching tool for connecting investigators with an interest in the same gene. Hum. Mutat. *36*, 928–930.
38. Tauriello, D.V.F., Jordens, I., Kirchner, K., Slootstra, J.W., Kruitwagen, T., Bouwman, B.A.M., Noutsou, M., Rüdiger, S.G.D., Schwamborn, K., Schambony, A., and Maurice, M.M. (2012). Wnt/β-catenin signaling requires interaction of the Dishevelled DEP domain and C terminus with a discontinuous motif in Frizzled. Proc. Natl. Acad. Sci. USA *109*, E812–E820.
39. Punchihewa, C., Ferreira, A.M., Cassell, R., Rodrigues, P., and Fujii, N. (2009). Sequence requirement and subtype specificity in the high-affinity interaction between human frizzled and dishevelled proteins. Protein Sci. *18*, 994–1002.
40. Saal, H.M., Prows, C.A., Guerreiro, I., Donlin, M., Knudson, L., Sund, K.L., Chang, C.F., Brugmann, S.A., and Stottmann, R.W. (2015). A mutation in FRIZZLED2 impairs Wnt signaling and causes autosomal dominant omodysplasia. Hum. Mol. Genet. *24*, 3399–3409.
41. McKusick, V.A. (1969). On lumpers and splitters, or the nosology of genetic disease. Perspect. Biol. Med. *12*, 298–312.
42. Boone, P.M., Campbell, I.M., Baggett, B.C., Soens, Z.T., Rao, M.M., Hixson, P.M., Patel, A., Bi, W., Cheung, S.W., Lalani, S.R., et al. (2013). Deletions of recessive disease genes: CNV contribution to carrier states and disease-causing alleles. Genome Res. *23*, 1383–1394.
43. Lalani, S.R., Liu, P., Rosenfeld, J.A., Watkin, L.B., Chiang, T., Leduc, M.S., Zhu, W., Ding, Y., Pan, S., Vetrini, F., et al. (2016). Recurrent muscle weakness with rhabdomyolysis, metabolic crises, and cardiac arrhythmia due to bi-allelic *TANGO2* mutations. Am. J. Hum. Genet. *98*, 347–357.
44. Harel, T., Yoon, W.H., Garone, C., Gu, S., Coban-Akdemir, Z., Eldomery, M.K., Posey, J.E., Jhangiani, S.N., Rosenfeld, J.A., Cho, M.T., et al.; Baylor-Hopkins Center for Mendelian Genomics; and University of Washington Center for Mendelian Genomics (2016). Recurrent de novo and biallelic variation of *ATAD3A*, encoding a mitochondrial membrane protein, results in distinct neurological syndromes. Am. J. Hum. Genet. *99*, 831–845.
45. Gu, S., Yuan, B., Campbell, I.M., Beck, C.R., Carvalho, C.M.B., Nagamani, S.C.S., Erez, A., Patel, A., Bacino, C.A., Shaw, C.A., et al. (2015). *Alu*-mediated diverse and complex pathogenic copy-number variants within human chromosome 17 at p13.3. Hum. Mol. Genet. *24*, 4061–4077.
46. Mayle, R., Campbell, I.M., Beck, C.R., Yu, Y., Wilson, M., Shaw, C.A., Bjergbaek, L., Lupski, J.R., and Ira, G. (2015). DNA REPAIR. Mus81 and converging forks limit the mutagenicity of replication fork breakage. Science *349*, 742–747.
47. Carvalho, C.M.B., and Lupski, J.R. (2016). Mechanisms underlying structural variant formation in genomic disorders. Nat. Rev. Genet. *17*, 224–238.
48. Kurooka, H., Kato, K., Minoguchi, S., Takahashi, Y., Ikeda, J., Habu, S., Osawa, N., Buchberg, A.M., Moriwaki, K., Shisa, H., and Honjo, T. (1997). Cloning and characterization of the nucleoredoxin gene that encodes a novel nuclear protein related to thioredoxin. Genomics *39*, 331–339.
49. Funato, Y., Terabayashi, T., Sakamoto, R., Okuzaki, D., Ichise, H., Nojima, H., Yoshida, N., and Miki, H. (2010). Nucleoredoxin sustains Wnt/β-catenin signaling by retaining a pool of inactive dishevelled protein. Curr. Biol. *20*, 1945–1952.
50. Boles, M.K., Wilkinson, B.M., Wilming, L.G., Liu, B., Probst, F.J., Harrow, J., Grafham, D., Hentges, K.E., Woodward, L.P., Maxwell, A., et al. (2009). Discovery of candidate disease genes in ENU-induced mouse mutants by large-scale sequencing, including a splice-site mutation in nucleoredoxin. PLoS Genet. *5*, e1000759.
51. Mazzeu, J.F., Pardono, E., Vianna-Morgante, A.M., Richieri-Costa, A., Ae Kim, C., Brunoni, D., Martelli, L., de Andrade, C.E., Colin, G., and Otto, P.A. (2007). Clinical characterization of autosomal dominant and recessive variants of Robinow syndrome. Am. J. Med. Genet. A. *143*, 320–325.
52. Habas, R., Dawid, I.B., and He, X. (2003). Coactivation of Rac and Rho by Wnt/Frizzled signaling is required for vertebrate gastrulation. Genes Dev. *17*, 295–309.
53. Bishop, J.R., Schuksz, M., and Esko, J.D. (2007). Heparan sulphate proteoglycans fine-tune mammalian physiology. Nature *446*, 1030–1037.
54. Campos-Xavier, A.B., Martinet, D., Bateman, J., Belluoccio, D., Rowley, L., Tan, T.Y., Baxová, A., Gustavson, K.H., Borochowitz, Z.U., Innes, A.M., et al. (2009). Mutations in the heparan-sulfate proteoglycan glypican 6 impair endochondral ossification and cause recessive omodysplasia. Am. J. Hum. Genet. *84*, 760–770.
55. Pilia, G., Hughes-Benzie, R.M., MacKenzie, A., Baybayan, P., Chen, E.Y., Huber, R., Neri, G., Cao, A., Forabosco, A., and Schlessinger, D. (1996). Mutations in *GPC3*, a glypican gene, cause the Simpson-Golabi-Behmel overgrowth syndrome. Nat. Genet. *12*, 241–247.
56. Ohkawara, B., Yamamoto, T.S., Tada, M., and Ueno, N. (2003). Role of glypican 4 in the regulation of convergent extension movements during gastrulation in *Xenopus laevis*. Development *130*, 2129–2138.
57. Tsuda, M., Kamimura, K., Nakato, H., Archer, M., Staatz, W., Fox, B., Humphrey, M., Olson, S., Futch, T., Kaluza, V., et al. (1999). The cell-surface proteoglycan Dally regulates Wingless signalling in Drosophila. Nature *400*, 276–280.
58. Waterson, J., Stockley, T.L., Segal, S., and Golabi, M. (2010). Novel duplication in glypican-4 as an apparent cause of Simpson-Golabi-Behmel syndrome. Am. J. Med. Genet. A. *152A*, 3179–3181.
59. Wiweger, M.I., Avramut, C.M., de Andrea, C.E., Prins, F.A., Koster, A.J., Ravelli, R.B.G., and Hogendoorn, P.C.W. (2011). Cartilage ultrastructure in proteoglycan-deficient zebrafish mutants brings to light new candidate genes for human skeletal disorders. J. Pathol. *223*, 531–542.
60. Allan, W. (1939). Relation of hereditary pattern to clinical severity as illustrated by peroneal atrophy. Arch. Intern. Med. (Chic.) *63*, 1123–1131.
61. Morton, N.E. (1956). The detection and estimation of linkage between the genes for elliptocytosis and the Rh blood type. Am. J. Hum. Genet. *8*, 80–96.
62. Sobreira, N.L., and Valle, D. (2016). Lessons learned from the search for genes responsible for rare Mendelian disorders. Mol. Genet. Genomic Med. *4*, 371–375.
63. Amberger, J.S., Bocchini, C.A., Schiettecatte, F., Scott, A.F., and Hamosh, A. (2015). OMIM.org: Online Mendelian Inheritance

in Man (OMIM®), an online catalog of human genes and genetic disorders. Nucleic Acids Res. *43*, D789–D798.
64. Brunner, H.G., and van Driel, M.A. (2004). From syndrome families to functional genomics. Nat. Rev. Genet. *5*, 545–551.
65. Qian, D., Jones, C., Rzadzinska, A., Mark, S., Zhang, X., Steel, K.P., Dai, X., and Chen, P. (2007). Wnt5a functions in planar cell polarity regulation in mice. Dev. Biol. *306*, 121–133.
66. Yamaguchi, T.P., Bradley, A., McMahon, A.P., and Jones, S. (1999). A Wnt5a pathway underlies outgrowth of multiple structures in the vertebrate embryo. Development *126*, 1211–1223.
67. Li, Y., and Dudley, A.T. (2009). Noncanonical frizzled signaling regulates cell polarity of growth plate chondrocytes. Development *136*, 1083–1092.
68. Schwabe, G.C., Trepczik, B., Süring, K., Brieske, N., Tucker, A.S., Sharpe, P.T., Minami, Y., and Mundlos, S. (2004). *Ror2* knockout mouse as a model for the developmental pathology of autosomal recessive Robinow syndrome. Dev. Dyn. *229*, 400–410.
69. Kuss, P., Kraft, K., Stumm, J., Ibrahim, D., Vallecillo-Garcia, P., Mundlos, S., and Stricker, S. (2014). Regulation of cell polarity in the cartilage growth plate and perichondrium of metacarpal elements by HOXD13 and WNT5A. Dev. Biol. *385*, 83–93.
70. Vinson, C.R., and Adler, P.N. (1987). Directional non-cell autonomy and the transmission of polarity information by the frizzled gene of Drosophila. Nature *329*, 549–551.
71. Klingensmith, J., Nusse, R., and Perrimon, N. (1994). The Drosophila segment polarity gene dishevelled encodes a novel protein required for response to the wingless signal. Genes Dev. *8*, 118–130.
72. Mikels, A.J., and Nusse, R. (2006). Purified Wnt5a protein activates or inhibits β-catenin-TCF signaling depending on receptor context. PLoS Biol. *4*, e115.
73. Bhanot, P., Brink, M., Samos, C.H., Hsieh, J.C., Wang, Y., Macke, J.P., Andrew, D., Nathans, J., and Nusse, R. (1996). A new member of the frizzled family from Drosophila functions as a Wingless receptor. Nature *382*, 225–230.
74. Sato, A., Yamamoto, H., Sakane, H., Koyama, H., and Kikuchi, A. (2010). Wnt5a regulates distinct signalling pathways by binding to Frizzled2. EMBO J. *29*, 41–54.
75. Sundaresan, M., Yu, Z.X., Ferrans, V.J., Irani, K., and Finkel, T. (1995). Requirement for generation of H_2O_2 for platelet-derived growth factor signal transduction. Science *270*, 296–299.
76. Hartmann, C., and Tabin, C.J. (2000). Dual roles of Wnt signaling during chondrogenesis in the chicken limb. Development *127*, 3141–3159.
77. Pan, W.J., Pang, S.Z., Huang, T., Guo, H.Y., Wu, D., and Li, L. (2004). Characterization of function of three domains in dishevelled-1: DEP domain is responsible for membrane translocation of dishevelled-1. Cell Res. *14*, 324–330.
78. Bernatík, O., Šedová, K., Schille, C., Ganji, R.S., Červenka, I., Trantírek, L., Schambony, A., Zdráhal, Z., and Bryja, V. (2014). Functional analysis of dishevelled-3 phosphorylation identifies distinct mechanisms driven by casein kinase 1ϵ and frizzled5. J. Biol. Chem. *289*, 23520–23533.
79. Ho, H.-Y.H., Susman, M.W., Bikoff, J.B., Ryu, Y.K., Jonas, A.M., Hu, L., Kuruvilla, R., and Greenberg, M.E. (2012). Wnt5a-Ror-Dishevelled signaling constitutes a core developmental pathway that controls tissue morphogenesis. Proc. Natl. Acad. Sci. USA *109*, 4044–4051.
80. Morita, K., Miyamoto, T., Fujita, N., Kubota, Y., Ito, K., Takubo, K., Miyamoto, K., Ninomiya, K., Suzuki, T., Iwasaki, R., et al. (2007). Reactive oxygen species induce chondrocyte hypertrophy in endochondral ossification. J. Exp. Med. *204*, 1613–1623.
81. McKusick, V.A. (2007). Mendelian Inheritance in Man and its online version, OMIM. Am. J. Hum. Genet. *80*, 588–604.
82. Boone, P.M., Yuan, B., Campbell, I.M., Scull, J.C., Withers, M.A., Baggett, B.C., Beck, C.R., Shaw, C.J., Stankiewicz, P., Moretti, P., et al. (2014). The Alu-rich genomic architecture of SPAST predisposes to diverse and functionally distinct disease-associated CNV alleles. Am. J. Hum. Genet. *95*, 143–161.
83. Boone, P.M., Liu, P., Zhang, F., Carvalho, C.M.B., Towne, C.F., Batish, S.D., and Lupski, J.R. (2011). *Alu*-specific microhomology-mediated deletion of the final exon of *SPAST* in three unrelated subjects with hereditary spastic paraplegia. Genet. Med. *13*, 582–592.
84. Trinh, T.Q., and Sinden, R.R. (1991). Preferential DNA secondary structure mutagenesis in the lagging strand of replication in *E. coli*. Nature *352*, 544–547.
85. Gonzaga-Jauregui, C., Harel, T., Gambin, T., Kousi, M., Griffin, L.B., Francescatto, L., Ozes, B., Karaca, E., Jhangiani, S.N., Bainbridge, M.N., et al.; Baylor-Hopkins Center for Mendelian Genomics (2015). Exome sequence analysis suggests that genetic burden contributes to phenotypic variability and complex neuropathy. Cell Rep. *12*, 1169–1183.
86. Wang, Y., Macke, J.P., Abella, B.S., Andreasson, K., Worley, P., Gilbert, D.J., Copeland, N.G., Jenkins, N.A., and Nathans, J. (1996). A large family of putative transmembrane receptors homologous to the product of the Drosophila tissue polarity gene frizzled. J. Biol. Chem. *271*, 4468–4476.

The American Journal of Human Genetics, Volume *102*

Supplemental Data

WNT Signaling Perturbations Underlie the Genetic Heterogeneity of Robinow Syndrome

Janson J. White, Juliana F. Mazzeu, Zeynep Coban-Akdemir, Yavuz Bayram, Vahid Bahrambeigi, Alexander Hoischen, Bregje W.M. van Bon, Alper Gezdirici, Elif Yilmaz Gulec, Francis Ramond, Renaud Touraine, Julien Thevenon, Marwan Shinawi, Erin Beaver, Jennifer Heeley, Julie Hoover-Fong, Ceren D. Durmaz, Halil Gurhan Karabulut, Ebru Marzioglu-Ozdemir, Atilla Cayir, Mehmet B. Duz, Mehmet Seven, Susan Price, Barbara Merfort Ferreira, Angela M. Vianna-Morgante, Sian Ellard, Andrew Parrish, Karen Stals, Josue Flores-Daboub, Shalini N. Jhangiani, Richard A. Gibbs, Baylor-Hopkins Center for Mendelian Genomics, Han G. Brunner, V. Reid Sutton, James R. Lupski, and Claudia M.B. Carvalho

Supplemental note: Case Reports

***WNT5A* CASE SUMMARIES**

BAB9138

BAB9138 is a seven year old boy born to parents with possible consanguinity. He has short stature (-4.25 SD), telecanthus, hypertelorism, frontal bossing, prominent eyes, anteverted nares, wide and depressed nasal bridge, midface hypoplasia, smooth philtrum, wide mouth, bilobed tongue, gingival hyperplasia, microretrognatia, and low-set ears. He has significant mesomelic limb shortening, and fingers and toes are very broad and short and nails are dysplastic. He had prior surgery to remove Y-shaped duplication of bilateral thumbs and great toes. He has a buried penis, cryptorchidism and sacral dimple. Radiographs revealed hemivertebrae (T6, T7, T13). Early motor milestones were delayed but present cognitive development is normal.

BAB9131

Subject BAB9131 is a 17 year old female. She was born at term with average birth parameters after an uncomplicated pregnancy to unrelated parents. She presented in infancy with slow linear growth marked by acromesomelia, hypertelorism and a prominent forehead. A clinical diagnosis of Robinow syndrome was made. By 18 months of age, height/length was 71.5 cm (-2.89 SD), weight was 9.15 kg (-1.97 SD), and high hyperopia was detected. She had normal motor, language and social development, delayed primary and secondary tooth eruption and dental crowding. By 8-3/4 years of age, height was 117 cm (-2.49 SD), weight was 25.8 kg (33%) and radiographs of the hands showed bifid tufts of the distal thumb. Research sequencing of *ROR2* was unrevealing though Robinow syndrome remained her clinical diagnosis. At 10 years of age she underwent bilateral distal tibial hemiepiphysiodesis and osteotomies for bilateral valgus ankle deformity and pain. This procedure improved her ankle pain, but she continued to have mild, diffuse pain of her hips, knees, elbows and shoulders, managed successfully with stretching and exercise. Menarche occurred at 12 years of age and was irregular until treated with OCPs. Laboratory evaluation to evaluate her irregular menses and hypertrichosis were normal. Multiple teeth were extracted and orthodontia implemented to align her teeth. In her mid teens, she began treatment for major depressive disorder. At her last encounter at 17 years of age, she was healthy and physically active without major medical concerns. Height was 144.5 cm (-2.85 SD) and weight was 48.5 kg (18%).

XpTER DELETION AND 6qTER DUPLICATION CASE SUMMARY

BAB8836

BAB8836 is a male and the third child of healthy Turkish parents who have consanguineous marriage. His brother and sister are healthy and there is no significant family history. He was born at term by vaginal delivery and was monitored for one week in neonatal period to reduce the levels of newborn bilirubin. At birth dysmorphic features were noted with short stature, large cranium, short neck, blue sclera, hypoplastic lower eyelids, flat nasal bridge, narrow rib cage, pectus carinatum, short arms and legs, and anal stenosis. After his second month, he developed xerosis. Milestones included unsupported sitting at 12-13 months, walking at 2 years old, and one word speaking at about 3-4 years; IQ measured at 8 years of age was 74. Echocardiography was normal and cranial MRI and abdominal ultrasound were also normal. Hemivertebra of T12 was noted radiographically and associated with kyphosis. He has post-natal short stature but weight is normal. Genetic testing revealed NM_0045603 p.R244W (c.730 C>T) (Heterozygote) alteration in the *ROR2* gene. Chromosome analysis was normal. Two large CNVs were observed in exome analysis by XHMM and HMZDelFinder and confirmed by aCGH: A terminal deletion on short arm of chromosome Xpter with approximate breakpoints (hg19) mapping in between chrX: 8,199,541 (min) chrX: 8,321,827 (max) and 6qter with approximate breakpoints mapping in between chr6:157,870,814 (min) and chr6:157,461,178 (max).

SH3PXD2B + *INPPL1* CASE SUMMARY

BAB8759

BAB8759 was a female born to consanguineous parents refered to genetics clinic at day of life 12 because of her facial dysmorphic features including prominent forehead, flat occiput, micrognathia, prominent eyes, hypertelorism, downslanting palpebral fissures, flat nasal bridge, nuchal edema and multiple congenital malformations, including pes equinovarus and atrioventricular septal defect. Chromosome analysis was normal. Her phenotypic features were said to be consistent with Robinow syndrome. This subject is deceased and had a history of recurrent respiratory infections. No radiologic imaging is available.

FZD2 CASE SUMMARIES

5449

Subject 5449 is a 10 year-old boy, second child of unrelated parents of Kosovoan origin. There is no family history of similar clinical findings. He was born at term after an uneventful pregnancy, and had normal birth parameters. He had several congenital anomalies that required surgical intervention, including imperforate anus, bilateral lacrimal duct agenesis, and thyroglossal duct cyst.

He also was noted to have bilateral chorioretinal colobomas, without associated visual impairment. Motor and cognitive development and growth have been normal.

His facial characteristics include a broad forehead, prominent eyes, hypertelorism with wide nasal bridge, hypoplasia of the nasal tip (almost bifid with midline telangiectasia) with anteverted nares, midface hypoplasia, posteriorly rotated and low set ears, and micrognathia. These facial features were considered compatible with Robinow syndrome. Anthropomorphic measurements revealed normal height, weight, and OFC, with also normal growth. Height was 137 cm (45th centile) and OFC 52.5 cm (-0.5 SD) at 10 years-old. Skeletal anomalies include mild mesomelia, bilateral short fibulas and ulna (with ulnar deviated hands and reduced wrist mobility), lower limb asymmetry, and proximally implanted thumbs. He has chronic ankle and wrist pain as a consequence of these ulnar and fibular anomalies. Dental anomalies are mild, consisting of teeth crowding.

Recurrent isolated headaches in the right temporal region prompted a brain CT-scan, which showed a type 1 Chiari malformation.

Chromosome analysis and array-CGH (180k Agilent) were normal. Whole exome sequencing identified a variant of unknown significance in *FZD2*, which matched with other subjects from the present study on GeneMatcher.

BAB8596

BAB8596 is a 6-year-old male born at full term via spontaneous vaginal delivery complicated by placental abruption requiring resuscitation for 13 minutes. His birth weight was 6lbs, 11oz (20^{th} centile) with a birth length of 18.25" (9^{th} centile) and a head circumference of 14" (45^{th} centile). He has had normal developmental milestones. He was referred to genetics for evaluation of skeletal dysplasia and had sequencing of *FGFR3* and *NPR2*. At 18 months of age, bone age was 33 months. Chromosomal microarray revealed a maternally-inherited 1q42.2 duplication that includes two genes that have not been associated with a clinical phenotype. At age 3yr 7mo, head circumference was 51.2 cm (78^{th} centile), height was 85.5 cm (-4 SD). Facial

characteristics include broad forehead, frontal bossing, depressed nasal bridge, anteverted nares, and midface hypoplasia. Brachydactyly and acromesomelic shortening of all extremities are present with a hand length of 9.7cm (<3rd centile) and middle finger length 3.9cm (<3rd centile).

BAB8594-affected mother of BAB8596

BAB8594 is the mother of BAB8596. She is 30-years-old from European origin. Her height is 4'11'' with a family history of short stature. There is no evidence of consanguinity. She has strabismus of her left eye. She has facial characteristics of Robinow syndrome and retrognathia. Hand length is 15.5 cm left and 15.7 cm right (<3rd centile).

BAB8705

BAB8705 is a 5-year-old female who was born at term with a birth weight of 3380 grams (39th centile) and height of 44 cm (1st centile). During the 6th month of pregnancy, ultrasound demonstrated short limbs. Prenatal chromosome and *FGFR3* mutation analyses performed on percutaneous umbilical cord blood sampling were normal. A clinical diagnosis of Robinow syndrome was rendered during the newborn period, based upon facial and limb characteristics. At 5 years of age, height is 94.5 cm (-2.9 SD), OFC is 48.5 cm (3-10th centile), she has facial characteristics of Robinow syndrome, 'V' shaped uvula, gingival hyperplasia, brachydactyly, mesomelia of upper limbs, genital hypoplasia and anteriorly-placed anus.

BAB7987

Subject BAB 7987 is a 15 year old female and was first evaluated at age three. Height is 4´10" (-2.25 SD); she has frontal bossing, midface hypoplasia, facial nevi, prominent eyes, upslanting palpebral fissures, long eyelashes, hypertelorism, short nose with anteverted nares, triangular mouth, accentuated cupids bow, micrognathia and multiple dental abnormalities. She has mesomelic limb shortening, with Madelung deformity, brachydactyly, clinodactyly and broad great toes. She has hypoplastic genitalia and recurrent urinary tract infections.

BAB7988-affected mother of BAB7987

Subject BAB 7988 is a 47 year old woman and is the mother of BAB7987. Her father is reported to be similarly affected, although he was unavailable for study. Her height is 5' (-1.7 SD); she has frontal bossing, midface hypoplasia, facial nevi, prominent eyes, upslanting palpebral fissures, strabismus, long eyelashes, hypertelorism, short nose with anteverted nares, triangular mouth, thin upper lip, cleft soft palate, bifid tongue, and dental abnormalities including supernumerary teeth. She has pectus excavatum, mesomelic limb shortening, with Madelung deformity, brachydactyly, short metacarpals, clinodactyly, broad great toes, and nail dysplasia. Her genitalia are hypoplastic and she has a small bladder.

BAB9254 & BAB9255

These are two siblings of BAB8596 who are 4 and 8 years of age. They have short stature, but are well and do not have facial characteristics of Robinow syndrome (all examined by author V.R.S.).

***NXN* CASE SUMMARIES**

BAB8841

BAB8841 is a 5-year-old female. Prenatal course was normal. Parents are first cousins of Turkish ancestry. At birth an omphalocele was present and was repaired in the first week of life. She has subsequently had two ventral hernias which were also repaired. Other medical concerns include bicuspid aortic valve with dilation of the ascending aorta (max Z-score of 2.0 at 5 months of life), aberrant right coronary artery, growth hormone deficiency (which was documented with a stimulation test and peak hormone level of 6.6 at 60 minutes), recurrent urinary tract infections and possible left kidney duplication, frequent ear infections, mild conductive hearing loss treated with two sets of ear tubes.

Growth parameters were normal at birth, but she developed short stature with relative macrocephaly; at 5 years of age, height was 2%, weight 9% and head circumference 100%. Craniofacial characteristics include a high and broad forehead, hypertrichosis with low anterior hairline, long eyelashes, hypertelorism, broad nasal bridge with anteverted nares, narrow posterior pharynx with absent uvula, gingival hyperplasia, midline groove and anterior notch in the tongue, notch in the upper lip in the midline, low set posteriorly rotated ears with cryptotia of the anterior helical rim. She has

brachydactyly and mesomelic shortening, fifth finger brachydactyly and clinodactyly and broad thumbs and great toes.

Development is delayed. She sat unassisted at 1 year of age, crawled at 18 months, pulled to stand at 30 months and walked at 36 months of age. She finger fed herself at 3 years and could copy a line and circle at 4 years. First word was at 1 year of age. She began to put words together into phrases at 5 years of age. She follows commands and communicates with some words as well as gestures, pointing. She has difficulty with pronunciation.

Chromosome analysis and chromosome microarray in 2011 were normal, and clinical sequencing and deletion/duplication analysis for *WNT5A*, *DVL1*, and *ROR2* were normal.

BAB9844

BAB9844 is a 3 year old girl who was born by caesarean section at 39 weeks gestation for breech presentation. She grew initially around the 25th centile for weight and height, and the 75th for head circumference. There was no concern about her general growth or development. She had an open fontanelle with a prominent metopic region, proptosis, a flat nasal bridge and flat midface with a tented upper lip and hypertrophic gums. She had a small jaw and no cleft. Although her overall length was in the normal range, she had the appearance of short limbs and she had an unusual pattern of hand and foot development with brachydactyly and incurving of her fingers towards the middle finger. There was a wide sandal gap and the same clinodactyly pattern in her feet. She had a nevus sebaceous on her scalp and no other malformation. She had a normal chromosome microarray analysis and Stickler syndrome was excluded clinically and following a panel of gene linked to the diagnosis. *ROR2* sequencing was normal.

BAB9847

BAB9847 is a 6 month old sibling of BAB9844 who was born at 37 weeks gestation by emergency caesarean section. A unilateral cleft lip and palate was detected antenatally, and she was thought to have the same facial profile as her sister. She has underdevelopment of her ear helices bilaterally. She is doing well. These siblings are otherwise remarkably alike in terms of their facial features and limb patterning and therefore exome sequencing was requested looking for a likely new recessive condition.

RAC3 CASE SUMMARY

BAB8740

BAB8740 is a 4-year-old female. She is the firstborn of healthy non-consanguineous parents delivered via cesarean section at 38 1/7 weeks gestation after an uneventful pregnancy. Her birth length was 48 cm (60^{th} centile), weight 3140 grams (55^{th} centile), and head circumference 34.5 cm (69^{th} centile). Current head circumference is 48 cm (5^{th} centile), length is 98 cm (5^{th} centile) and weight is 15 kg (17^{th} centile). An EEG was performed because of irritability and sharp waves were noted in left hemispheric region, seizures were observed and treated with valproic acid (150 ml/day). Brain MRI revealed a thin corpus callosum. Gross motor development was delayed and she did not achieve head control until 4 months, did not sit without support until 9-10 months and walked at age of 21 months. At four years of age she only says a few single words.

GPC4 CASE SUMMARY

BAB8295

BAB8295 is an 8-year old male. He was a 5-pound-4-ounce (89^{th} centile) product of a 33 week gestation delivered via SVD to 24-year-old G2, P1>2 and 24-year-old father. There were multiple medical issues at birth including choanal atresia, cleft palate, patent ductus arteriosus, grade 2/3 intraventricular hemorrhage, foramen magnum stenosis resulting in palsy of cranial nerves III, VI and VII. Breathing and feeding issues resulted in tracheostomy and gastrostomy tube placement with Nissen fundoplication. He also had recurrent infections managed with IVIG as well as multiple surgeries for the aforementioned birth defects as well as VP shunt placement. Radiographs at that time noted increased skull density and long bone striations. He is presently in 3^{rd} grade in regular classes and makes As. His weight is 23.9 kg (17%), height 115.1 cm (-2.88 SD) and OFC 60.2 cm (+5 SD). He has frontal bossing with a broad forehead, hypertelorism and telecanthus with downslanting palpebral fissures, low nasal bridge, anteverted nares, low-set ears, flat midface, cupid bow mouth, gingival hyperplasia, tracheostomy in place, mesomelia, brachydactyly with spatulated finger tips, broad thumbs and great toes and second toes that are medially deviated. External genitalia were normal. Detailed neuropsychological testing at 7 years of age revealed “average” scores on a variety of standardized tests. DEXA scan at 8 years of age revealed significant cranial sclerosis: Subtotal body (without head) BMC 457.00 g, BMD 0.616 g/cm^2, Z-score -1.0;

head BMC 847.64 g, BMD 2.974 g/cm^2; total body (with head) BMC 1304.64 g, BMD 1.270 g/cm^2, Z-score +9.4.

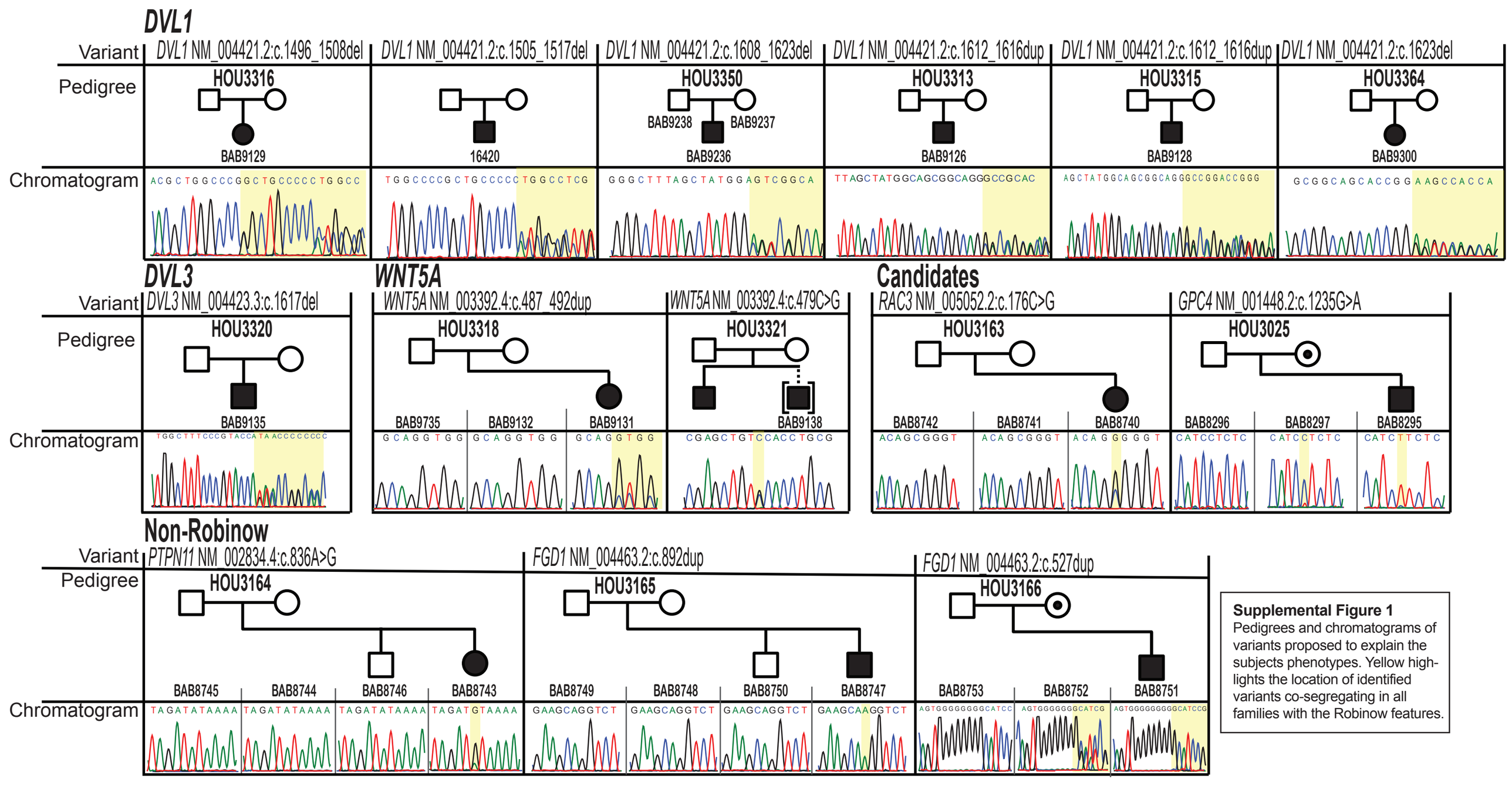

Supplemental Figure 1
Pedigrees and chromatograms of variants proposed to explain the subjects phenotypes. Yellow highlights the location of identified variants co-segregating in all families with the Robinow features.

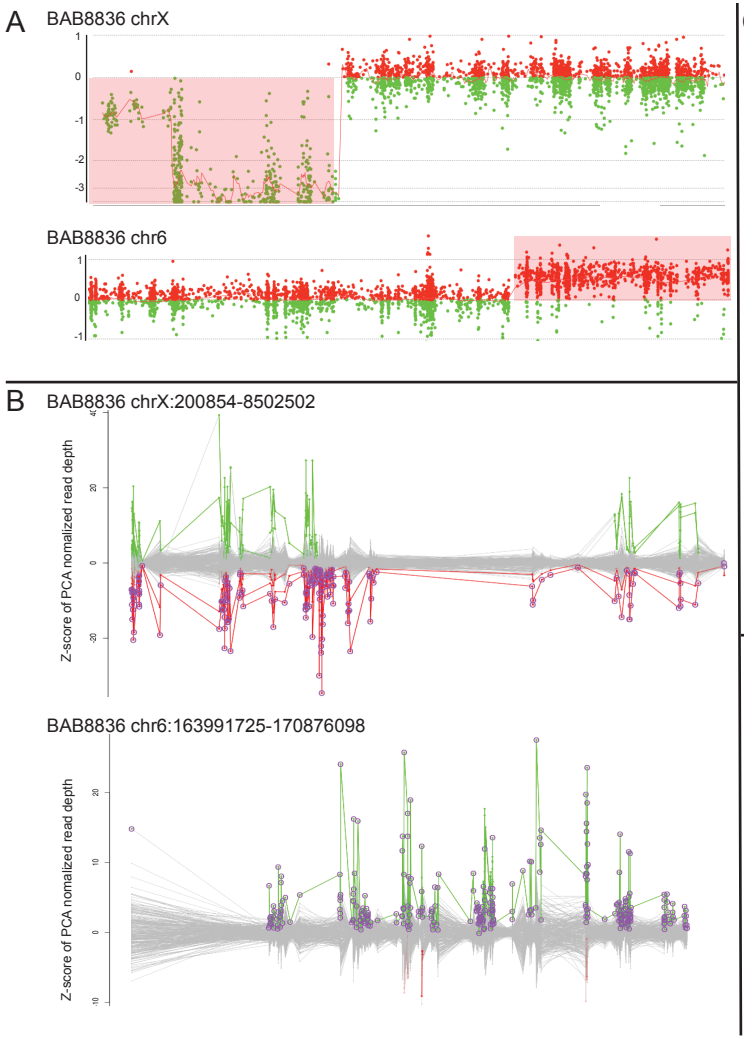

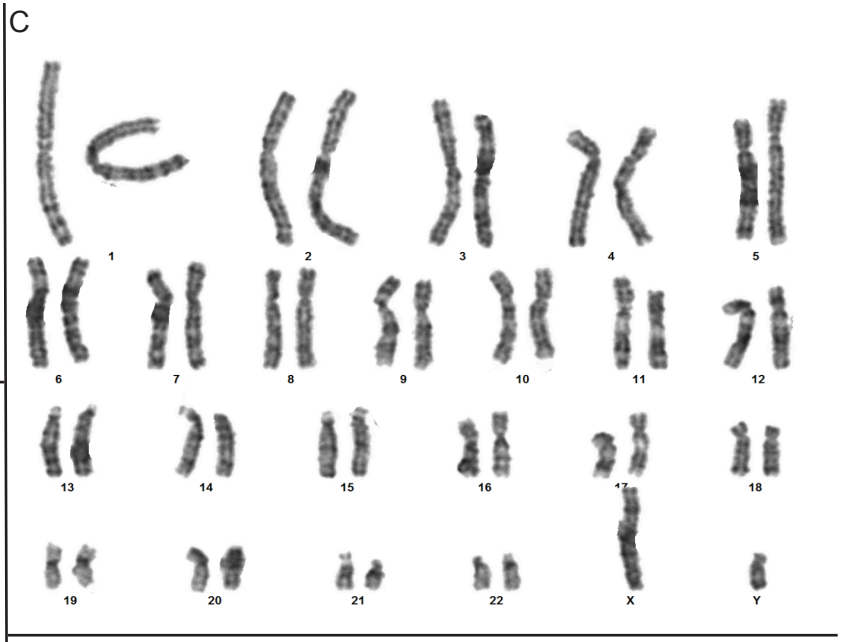

Supplemental Figure 2

Distinct methodologies used to identify copy-number alterations in BAB8836. A) High-density arrayCGH highlighting a terminal Xp deletion that spans chrX:409876-8199541(min) or chrX:der-8321827(max). A terminal 6q duplication is also observed that spans chr6:157870814-170881475 (min) or chr6:157461178-ter (max). B) XHMM plots identified from exome normalized read-depths showing CNVs in BAB8836. C) Karyotype of BAB8836 with 700 band resolution with a possible derivative X chromosome 46,XY,der(X)t(X,6)(p22.31;q25.3). arr[GRCh37]6q25.3q27(157,870,814_ 170,881,475)x3, Xp22.33p22.31(409,876_8,199,541)x0

5449

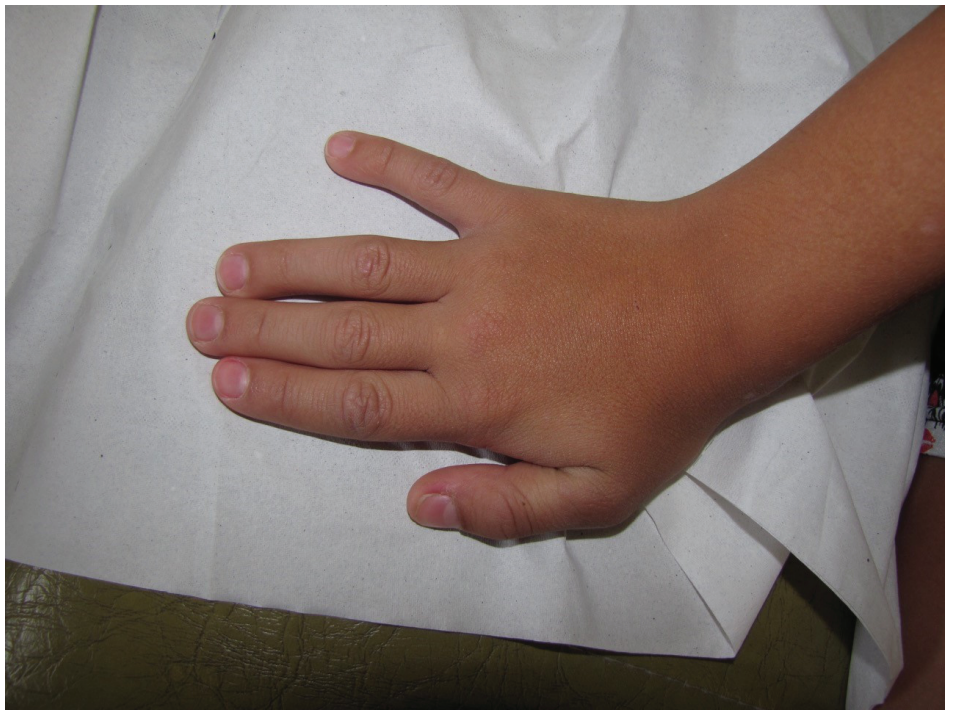

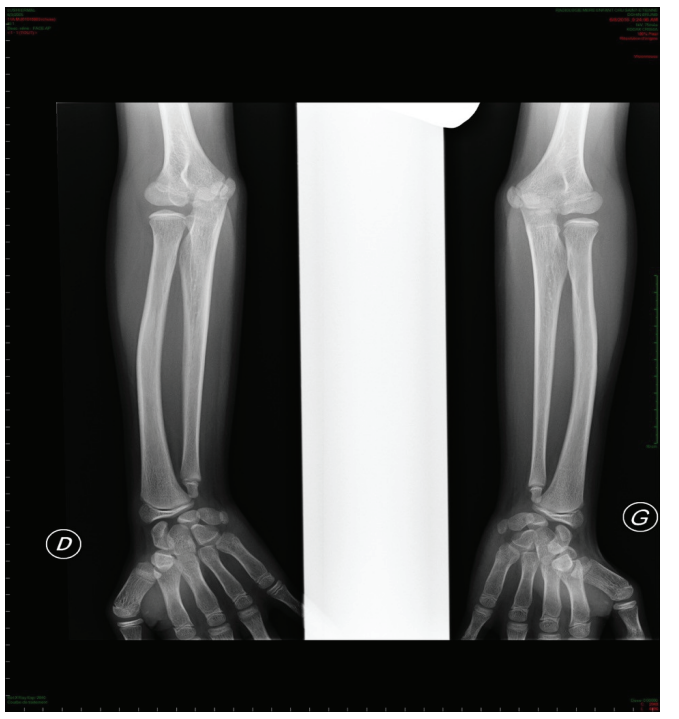

BAB8705

BAB8596

Supplemental Figure 3
Photos and radiographs of available individuals with variants in *FZD2*

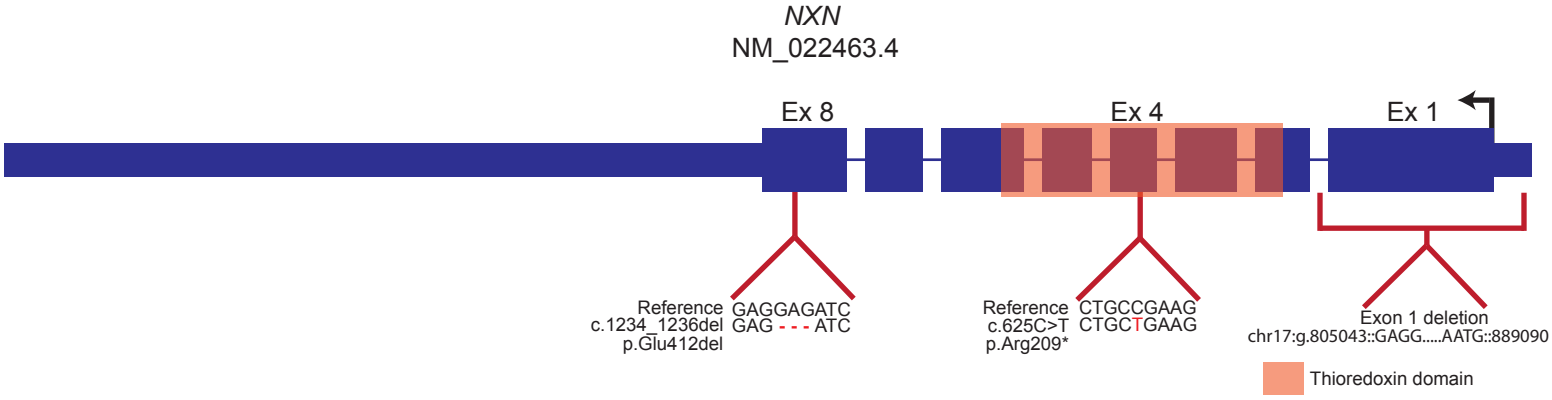

Supplemental Figure 4

Locations of the three distinct variants identified in the coding region of *NXN* according to the RefSeq transcript NM_022463.4. Orange box indicates the predicted thioredoxin domain of the resulting protein structure.

Supplemental table 1: Variants reported in this study

Individual ID	Secondary ID	Origin	Relationship	Gene	variant type	Zygosity	Transcript	cds_variant	p_variant	OMIM_phenotype
BAB9126	-	in-house cohort	Affected	*DVL1*	-1 frameshift	Heterozygous	NM_004421.2	c.1612_1616dup	p.Ser539Argfs*112	Robinow syndrome, Autosomal Dominant 2, 616331
BAB9128	-	in-house cohort	Affected	*DVL1*	-1 frameshift	Heterozygous	NM_004421.2	c.1612_1616dup	p.Ser539Argfs*112	Robinow syndrome, Autosomal Dominant 2, 616331
BAB9300	-	in-house cohort	Affected	*DVL1*	-1 frameshift	Heterozygous	NM_004421.2	c.1623del	p.Ser542Valfs*107	Robinow syndrome, Autosomal Dominant 2, 616331
BAB9129	-	in-house cohort	Affected	*DVL1*	-1 frameshift	Heterozygous	NM_004421.2	c.1496_1508del	p.Pro499Argfs*146	Robinow syndrome, Autosomal Dominant 2, 616331
16420	-	in-house cohort	Affected	*DVL1*	-1 frameshift	Heterozygous	NM_004421.2	c.1505_1517del	p.His502Profs*143	Robinow syndrome, Autosomal Dominant 2, 616331
BAB9236	-	in-house cohort	affected	*DVL1*	-1 frameshift	Heterozygous	NM_004421.2	c.1608_1623del	p.Ser537Valfs*107	Robinow syndrome, Autosomal Dominant 2, 616331
BAB9135	-	in-house cohort	Affected	*DVL3*	-1 frameshift	Heterozygous	NM_004423.3	c.1617del	p.Gln539Hisfs*129	Robinow syndrome, Autosomal Dominant 3, 616894
BAB 7987	BH9272_1	in-house cohort	Affected	*FZD2*	missense	Heterozygous	NM_001466.3	c.1301G>T	p.Gly434Val	NA
BAB 7988	BH9272_2	in-house cohort	Affected mother of BAB7987	*FZD2*	missense	Heterozygous	NM_001466.3	c.1301G>T	p.Gly434Val	NA
BAB8594	BH8637_3	in-house cohort	affected mother of BAB8596	*FZD2*	Nonsense	Heterozygous	NM_001466.3	c.1130G>A	p.Trp377*	NA
BAB8596	BH8637_1	in-house cohort	affected	*FZD2*	Nonsense	Compound Heterozygous	NM_001466.3	c.1130G>A c.425C>T	p.Trp377* p.Pro142Leu	NA
BAB8705	BH8808_1	in-house cohort	affected	*FZD2*	missense	Heterozygous	NM_001466.3	c.1301_1302delinsTT	p.Gly434Val	NA
BAB8295	BH7859_1	in-house cohort	affected	*GPC4*	missense	hemizygous	NM_001448.2	c.1235G>A	p.Arg412Lys	NA
BAB9138	BH9278_1	in-house cohort	affected	*WNT5A*	missense	Heterozygous	NM_003392.4	c.479C>G	p.Ser160Cys	Robinow syndrome, Autosomal Dominant 1, 180700
BAB9131	BH9276_1	in-house cohort	Affected	*WNT5A*	nonframeshift insertion	Heterozygous	NM_003392.4	c.487_492dup	p.Gly163_Cys164dup	Robinow syndrome, Autosomal Dominant 1, 180700
BAB8759	BH9282_1	in-house cohort	affected	*INPPL1;SH3PXD2B*	Missense; Frameshift deletion	Homozygous(2)	NM_001567.3, NM_001017995.2	c.1636G>A;c.969del	p.Val546Ile; p.Arg324Glyfs*19	Opsismodysplasia, 258480; Frank-ter Haar syndrome, 249420
BAB8841	BH9279_1	in-house cohort	affected	*NXN*	Nonsense	Homozygous	NM_022463.4	c.625C>T	p.Arg209*	NA
BAB8747	BH8811_1	in-house cohort	affected	*FGD1*	Frameshift insertion	Hemizygous	NM_004463.2	c.892dup	p.Cys298Leufs*5	Aarskog-Scott syndrome, 305400
BAB8751	BH9281_1	in-house cohort	affected	*FGD1*	Frameshift insertion	Hemizygous	NM_004463.2	c.527dup	p.Leu177Thrfs*40	Aarskog-Scott syndrome, 305400
BAB8743	BH8812_1	in-house cohort	affected	*PTPN11*	missense	Heterozygous	NM_002834.4	c.836A>G	p.Tyr279Cys	Noonan syndrome, 163950
BAB8740	BH9280_1	in-house cohort	affected	*RAC3*	missense	Heterozygous	NM_005052.2	c.176C>G	p.Ala59Gly	NA
BAB9127	BH9274_1	in-house cohort	affected	NA	NA	NA		NA		NA
BAB8836	BH10050_1	in-house cohort	affected	NA	CNV	Hemizygous; Heterozygous	NA	46,XY,der(X)t(X;6)(p22.31;q25.3).arr[GRCh37]6q25.3q27(157,870,814_170,881,475)x3, Xp22.33p22.31(409,876_8,199,541)x0	NA	NA
5449	-	GeneMatcher	Affected	*FZD2*	missense	Heterozygous	NM_001466.3	c.1300G>A	p.Gly434Ser	NA
BAB9844	UK1	GeneMatcher	Affected	*NXN*	Nonframeshift deletion, CNV	Compound heterozygous	NM_022463.4	c.1234_1236del; chr17:g.805043::GAGG.....AATG::889090	p.Glu412del,???	NA
BAB9847	UK2	GeneMatcher	Affected	*NXN*	Nonframeshift deletion, CNV	Compound heterozygous	NM_022463.4	c.1234_1236del; chr17:g.805043::GAGG.....AATG::889090	p.Glu412del,???	NA

Supplemental table 2: Variants reported in the literature

Individual ID	Origin	Gene	Transcript	cds_variant	p_variant	OMIM_phenotype
family 1	Roifman et al 2015	*WNT5A*	NM_003392.4	c.257A>G	p.Tyr86Cys	Robinow syndrome, Autosomal Dominant 1, 180700
family 2	Roifman et al 2015	*WNT5A*	NM_003392.4	c.206G>A	p.Cys69Tyr	Robinow syndrome, Autosomal Dominant 1, 180700
family 3	Roifman et al 2015	*WNT5A*	NM_003392.4	c.257A>G	p.Tyr86Cys	Robinow syndrome, Autosomal Dominant 1, 180700
-	Person et al 2010	*WNT5A*	NM_003392.4	c.248G>C	p.Cys83Ser	Robinow syndrome, Autosomal Dominant 1, 180700
-	Person et al 2010	*WNT5A*	NM_003392.4	c.544_545delinsTC	p.Cys182Arg	Robinow syndrome, Autosomal Dominant 1, 180700
-	Saal et al 2015	*FZD2*	NM_001466.3	c.1644G>A	p.Trp548*	NA
BAB4073	White et al 2015	*DVL1*	NM_004421.2	c.1570_1571delins	p.Phe524Profs*125	Robinow syndrome, Autosomal Dominant 2, 616331
BAB4878	White et al 2015	*DVL1*	NM_004421.2	c.1505_1517del	p.His502Profs*143	Robinow syndrome, Autosomal Dominant 2, 616331
BAB5264	White et al 2015	*DVL1*	NM_004421.2	c.1519del	p.Trp507Glyfs*142	Robinow syndrome, Autosomal Dominant 2, 616331
016462	White et al 2015	*DVL1*	NM_004421.2	c.1505_1517del	p.His502Profs*143	Robinow syndrome, Autosomal Dominant 2, 616331
016516	White et al 2015	*DVL1*	NM_004421.2	c.1508del	p.Pro503Argfs*146	Robinow syndrome, Autosomal Dominant 2, 616331
017604	White et al 2015	*DVL1*	NM_004421.2	c.1615del	p.Ser539Alafs*110	Robinow syndrome, Autosomal Dominant 2, 616331
030526	White et al 2015	*DVL1*	NM_004421.2	c.1529del	p.Gly510Valfs*139	Robinow syndrome, Autosomal Dominant 2, 616331
Subject 1	Bunn et al 2015	*DVL1*	NM_004421.2	c.1519del	p.Trp507Glyfs*142	Robinow syndrome, Autosomal Dominant 2, 616331
Subject 2	Bunn et al 2015	*DVL1*	NM_004421.2	c.1562del	p.Pro521Hisfs*128	Robinow syndrome, Autosomal Dominant 2, 616331
Subject 3	Bunn et al 2015	*DVL1*	NM_004421.2	c.1576_1583delinsG	p.Pro526Alafs*121	Robinow syndrome, Autosomal Dominant 2, 616331
BAB8062	White et al 2016	*DVL1*	NM_004421.2	c.1522del	p.Pro508Leufs*141	Robinow syndrome, Autosomal Dominant 2, 616331
015902	White et al 2016	*DVL3*	NM_004423.3	c.1749del	p.Ser583Argfs*85	Robinow syndrome, Autosomal Dominant 3, 616894
BAB7990	White et al 2016	*DVL3*	NM_004423.3	c.1585del	p.Ala529Profs*139	Robinow syndrome, Autosomal Dominant 3, 616894
BAB7985	White et al 2016	*DVL3*	NM_004423.3	c.1715-2A>G	p.?	Robinow syndrome, Autosomal Dominant 3, 616894
BAB7982	White et al 2016	*DVL3*	NM_004423.3	c.1715-1G>A	p.?	Robinow syndrome, Autosomal Dominant 3, 616894
BAB4569	White et al 2016	*DVL3*	NM_004423.3	c.1716del	p.Ser573Valfs*95	Robinow syndrome, Autosomal Dominant 3, 616894